



Mathematical analysis and prediction of future outbreak of dengue on time-varying contact rate using machine learning approach

Md Shahidul Islam^{a,b,d}, Pabel Shahrear^{b,*}, Goutam Saha^c, Md Ataullha^d, M. Shahidur Rahman^d

^a Department of Computer Science and Engineering, Green University of Bangladesh, Kanchon, 1460, Bangladesh

^b Department of Mathematics, Shahjalal University of Science and Technology, Sylhet, 3114, Bangladesh

^c Department of Mathematics, University of Dhaka, Dhaka, 1000, Bangladesh

^d Department of Computer Science and Engineering, Shahjalal University of Science and Technology, Sylhet, 3114, Bangladesh

ARTICLE INFO

Keywords:

Basic reproduction number
Dengue
Machine learning
Time-series forecasting
Awareness
Prophet model

ABSTRACT

This article introduces a novel mathematical model analyzing the dynamics of Dengue in the recent past, specifically focusing on the 2023 outbreak of this disease. The model explores the patterns and behaviors of dengue fever in Bangladesh. Incorporating a sinusoidal function reveals significant mid-May to Late October outbreak predictions, aligning with the government's exposed data in our simulation. For different amplitudes (A) within a sequence of values ($A = 0.1$ to 0.5), the highest number of infected mosquitoes occurs in July. However, simulations project that when $\beta_M = 0.5$ and $A = 0.1$, the peak of human infections occurs in late September. Not only the next-generation matrix approach along with the stability of disease-free and endemic equilibrium points are observed, but also a cutting-edge Machine learning (ML) approach such as the Prophet model is explored for forecasting future Dengue outbreaks in Bangladesh. Remarkably, we have fitted our solution curve of infection with the reported data by the government of Bangladesh. We can predict the outcome of 2024 based on the ML Prophet model situation of Dengue will be detrimental and proliferate 25 % compared to 2023. Finally, the study marks a significant milestone in understanding and managing Dengue outbreaks in Bangladesh.

1. Introduction

Dengue incidence (DI) in 2023 in Bangladesh has shattered records dating back 22 years, signaling a dire public health crisis. The significant increase in confirmed Dengue cases implies that the virus is spreading more vigorously and rapidly than in recent history. DI began to rise significantly starting in May, with 1036 cases. This trend continued throughout the summer months, reaching an alarming peak of 71,976 cases in August. The notable increase in Dengue cases is worrisome and raises the possibility of a severe outbreak later this year.

The Aedes mosquito plays a pivotal role in the transmission of the Dengue virus, posing a substantial threat to human health and exerting a profound impact on the demographics and socio-economic aspects of numerous tropical and subtropical regions. Despite strenuous efforts by scientists, finding a definitive solution for this virus remains a

formidable challenge, primarily because it hinges on various factors, including environmental considerations and societal awareness. In 2005, Hoffmann [1] introduced a scientific approach based on Cytoplasmic Incompatibility (CI) as a potential means to combat the virus. This approach involves infecting the *Culex pipiens* mosquito with Wolbachia bacteria, which reside within the host's reproductive cells, thereby impairing offspring production when strains of the same species are infected.

Sangkaew et al. [2] conducted a study on the spread of various diseases caused by Dengue. In this study, key factors contributing to the progression of Dengue were identified during the febrile period. The study revealed a higher vulnerability among female patients. Additionally, it highlighted the critical nature of the first phase when proper treatment is not administered, potentially leading to life-threatening consequences. Notably, Serotype-2 was identified as a major culprit

Abbreviations: ARIMA, Autoregressive Integrated Moving Average; LSTM, Long Short-Term Memory; CI, Cytoplasmic incompatibility; DI, Dengue incidence; DI, Dengue Infections; E, Exposed; SARIMAX, Seasonal Auto Regressive Integrated Moving Average; I, Infected; R, Recovered; S, Susceptible; H, Human; M, Mosquito; ML, Machine learning.

* Corresponding author.

E-mail address: shahrear-mat@sust.edu (P. Shahrear).

<https://doi.org/10.1016/j.compbioemed.2024.108707>

Received 11 November 2023; Received in revised form 14 May 2024; Accepted 3 June 2024

Available online 4 June 2024

0010-4825/© 2024 Published by Elsevier Ltd.

for associated diseases in children. Furthermore, it is observed that secondary infections tended to advance more rapidly in children compared to those associated with Serotype-1 or Serotype-3. The intensity of Dengue is responsible for climate change and aimless urbanization based on constructions and unrealistic projects funded by corporations with the aid of different financing authorities. The government somehow didn't address the healthcare system's development; because of that, when any disease emerges, the situation was out of control in a few days. Moreover, the lack of government and private hospitals and efficient staff of medical doctors and clinical professionals also amplified the hostile situations once the disease commenced. A few of that was addressed by Hasan et al. [3].

Wilder-Smith et al. [4–6] have focused on the development of vaccines for Dengue and its priorities on public health. It is reported that the first-ever appearance of the Dengue vaccine was in 2015, but it depends on serotype. Banu et al. [7] carried out an exhaustive analysis to examine the repercussions of meteorological variability on the dissemination of Dengue fever in Dhaka, Bangladesh during 2000–2010. This study's findings established a robust affirmative correlation between meteorological parameters, such as temperature and atmospheric moisture levels, and the proliferation of Dengue transmission.

Numerous studies have been conducted in various countries to investigate the factors of Dengue Infection (DI). According to Sharmin et al. [8], temperature, rainfall, and population density were substantially linked with DI transmission in Dhaka, Bangladesh. Muurink et al. [9] implemented a data mining methodology to predict long-term Dengue outbreaks in Bangladesh. Their discovery is fascinating because the key environmental components are identified. The cumulative number of rainy days, the minimum daily temperature, and the average humidity levels were the best predictors of these outbreaks. Dyer [10] documented a Dengue epidemic in the Philippines in 2019, with 98 % more cases and fatalities compared to 2018. Kong et al. [11] studied the potential environmental and socioeconomic factors of DI in Guangzhou, China, from 2006 to 2014. They uncovered that DI was significantly influenced by rainfall, precipitation, temperature, population density, and geographical distribution.

Hossain et al. [12] used the ARIMA model to assess daily temperature, rainfall, and DI data in order to study the 2019 Dengue outbreaks in Dhaka, Bangladesh. They identified a significant connection between the Dengue outbreak in Dhaka and the condition elsewhere in the nation, which they attributed to a large-scale exodus of residents from Dhaka during the Eid holiday. Islam et al. [13] explored the relationship between climate variables and DI in Dhaka, Bangladesh, from 2002 to 2013. Their analysis revealed a strong association between rising temperatures, increased humidity, and greater rainfall with DI. Xavier et al. [14] examined the correlation between climate parameters and the incidence of Dengue fever in Rio de Janeiro, Brazil. The data encompassed the years 2007–2016, revealing that both temperature and humidity emerged as significant contributors to the spread of Dengue fever. Manna et al. [15] examined the transmission of Dengue and strategies for its mitigation in countries like Bangladesh, Pakistan, India, Nepal, Sri Lanka, and Afghanistan, within the timeframe of 2018–2021. They emphasized the need for heightened focus on controlling Dengue outbreaks, particularly during the COVID-19 era.

Naher et al. [16] utilized time-series analysis and research data spanning from 2008 to 2020 to make short-term predictions regarding DI in Bangladesh. Through a thorough examination of various models, they determined that the ARIMA model outperformed others in terms of prediction accuracy. Importantly, their findings suggest a trend toward increased DI in Bangladesh in the future. Aldila et al. [17] introduced an innovative mathematical model comprising both human (SAEHR) and mosquito (SI) components. This research is based on DI in Jakarta in 2020. It is found that DI case detection holds little sway in mitigating Dengue transmission. However, a pivotal element for diminishing the spread of Dengue lies in bolstering individuals' consciousness.

Hossain et al. [18] conducted a statistical investigation aimed at

elucidating the link between environmental factors and the occurrence of Dengue fever in Dhaka, Bangladesh, spanning the years from 2013 to 2020. Their findings reveal strong positive correlations DI and maximum and minimum temperatures, humidity, and wind speed. Conversely, they identified negative correlations between DI and both rainfall and sunshine levels. Islam et al. [19] investigated the correlation between DI and environmental elements within the timeframe spanning from 2000 to 2023, focusing on the context of Bangladesh. The study took into account various meteorological parameters, including temperature, humidity, precipitation, surface pressure, and wind speed. The findings revealed a robust association between temperature and rainfall, which consistently influenced the year-round spread of Dengue.

The basic reproductive ratio (R_0) is a pivotal factor used to measure the possibility of spreading disease in a group of people. Here, $R_0 > 1$ suggests that the disease can continue transmission within the susceptible population, leading to an epidemic or endemic state. Whereas $R_0 < 1$ suggests that the disease will die out over time. It is important to note that R_0 offers a theoretical estimation based on the assumption that of a susceptible class and may not comprehensively account for real-world complexities such as immunity, vaccination etc. To estimate R_0 , Jafaruddin et al. (2015) proposed two different approaches and suggested that considering the existence of infected mosquitoes during the initial growth phase of an infected human was a more realistic approach [20]. Later, Brauer et al. (2016) introduced two epidemic models specifically designed for Dengue and the Zika virus [21]. Their analysis considered the initial exponential growth rate as a basis for estimating R_0 . The study revealed an approximate value of R_0 of 2.03 in temperate zones, 3.44 in tropical zones, and 10.29 in subtropical zones. Mordecai et al. (2019) examine the thermal biology of mosquito-borne disease [22]. They investigate how temperature influences the transmission dynamics of diseases such as dengue fever. The authors interpret various factors in different temperature regimes, including mosquito physiology, pathogen development, and vector competence. This study enhances the predictability of models and informs public health interventions about the thermal constraints on disease transmission.

For the first time, Delamater et al. (2019) thoroughly explored the conceptual traces of R_0 , shedding light on its details [23]. They emphasized R_0 as a pivotal epidemiological concept, stressing its mathematical calculation based on the model's structure. They also pointed out that while R_0 is a valuable metric for estimating contagiousness, it does not convey information about the severity of infectious diseases. O'Reilly et al. (2019) estimated the burden of dengue fever and the potential impact of releasing Wolbachia-infected mosquitoes in Indonesia [24]. Moreover, they inaugurated sophisticated modeling techniques to project the spread of dengue and assess the efficacy of Wolbachia-infected mosquitoes in disease control. This study nourishes insights into the potential benefits of novel vector control strategies in mitigating dengue fever in society. In 2020, Liu et al. (2020) conducted a literature review, providing diverse estimates of R_0 across various climate zones [25]. Pereira and Schmit (2022) examine the spatial dynamics of dengue fever transmission in Sao Paulo, Brazil [26]. The study investigated the coexistence of two dengue serotypes and their spatial spread within the city. Through mathematical modeling, the authors elucidate how environmental factors and human mobility contribute to the propagation of dengue for urban disease control strategies.

In this article, we have implemented a time-dependent transmission rate for humans induced by mosquitoes. This intimation reveals a significant milestone in understanding the acquisition of dengue outbreaks in Bangladesh. This is because the data on Bangladesh is available to us apart from the dengue situations in nearby southeast Asian countries. Practical analysis gives us information about the reliability of the proposed new model. We also yield attention to predicting the outbreak in advance based on machine-learning forecasting. To the best of our knowledge, execution of such inclusion is hardly found in existing studies. These two significantly contribute to assimilating and

understanding the Dengue situation and warn us about the future of this deadly disease.

The article is structured as follows: Following the introduction, the model is comprehensively explained. We then establish a foundation for rigorous stability analysis by proving fundamental theorems regarding positivity and boundedness. This analysis encompasses both the disease-free and endemic equilibria, culminating in the demonstration of the local asymptotic stability of the disease-free equilibrium. Next, we delve into global stability and its associated theorems. Moving forward, we conduct sensitivity analysis and utilize the findings to perform numerical simulations, illustrating the impacts of various parameters. Additionally, a machine learning approach is employed to predict future Dengue outbreaks in Bangladesh. Finally, the article concludes by summarizing the findings and citing references.

2. Model description

Let us consider a model with three compartments for mosquitoes: susceptible (S_M), infected (I_M), and recovered (R_M) and four compartments for humans: susceptible (S_H), exposed (E_H), infected (I_H), and recovered (R_H). When a mosquito bites a human, the human moves to the exposed class at a time dependent rate $\beta_H(t)$. After a certain duration, the human becomes affected by Dengue disease and transitions to the infected class at a rate α . After some more time, the human undergoes treatment and progresses to the recovered class at a rate γ . On the other hand, if a mosquito bites a human who is already infected due to previous mosquito bite, the mosquito transitions from the suspected class to the infected class at a rate β_M . After a period of time, the mosquito recovers from the infected class at a rate δ .with initial conditions

$$(S_H(0), E_H(0), I_H(0), S_M(0), I_M(0), R_M(0)) = (S_{H_0}, E_{H_0}, I_{H_0}, R_{H_0}, S_{M_0}, I_{M_0}, R_{M_0}) \quad (1b)$$

where $S_{H_0}, E_{H_0}, I_{H_0}, R_{H_0}, S_{M_0}, I_{M_0}, R_{M_0} \geq 0$.

A flow diagram of the system (1a) is presented in Fig. 1. List of

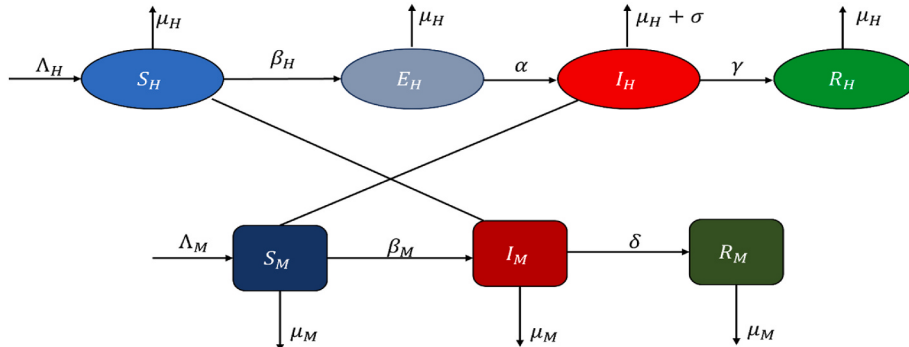


Fig. 1. Flow diagram of the proposed model.

$$\begin{aligned} \frac{dS_H}{dt} &= \Lambda_H - \beta_H(t)S_HI_M - \mu_H S_H \\ \frac{dE_H}{dt} &= \beta_H(t)S_HI_M - \alpha E_H - \mu_H E_H \\ \frac{dI_H}{dt} &= \alpha E_H - \gamma I_H - \mu_H I_H - \sigma I_H \\ \frac{dR_H}{dt} &= \gamma I_H - \mu_H R_H \\ \frac{dS_M}{dt} &= \Lambda_M - \beta_M S_M I_H - \mu_M S_M \\ \frac{dI_M}{dt} &= \beta_M S_M I_H - \delta I_M - \mu_M I_M \\ \frac{dR_M}{dt} &= \delta I_M - \mu_M R_M \end{aligned} \quad (1a)$$

parameters and its estimated values are presented in Table 1 (see Fig. 2 as a graphical representative).

3. Theoretical analysis

In this section, the basic properties of the proposed system will be examined, encompassing non-negativity, uniform boundedness, and the stability of both the disease-free equilibrium (DFE) and endemic equilibrium (EE). Additionally, an assessment of the basic reproduction number (R_0) will be conducted, along with an analysis of the local and global stability of the DFE and EE.

4. Basic properties of the proposed model

Firstly, the uniform boundedness criteria of the solutions of the proposed Dengue model must be examined to analyze its dynamics [29]. This involves verifying the positivity of the solutions, which means ensuring that all solutions of the Dengue model remain positive when initiated with nonnegative initial conditions. To demonstrate non-negativity and boundedness, two essential theorems shall be presented.

Theorem 1. All solutions of the proposed, dengue, model is nonnegative for any time t satisfying nonnegative initial conditions.

Proof: To prove this, we first show that $S_H(t) > 0$ for all time t . From Eq. (1a), we get,

$$\frac{dS_H}{dt} \geq -\beta_H(t)S_HI_M - \mu_H S_H \Rightarrow \frac{1}{S_H} \frac{dS_H}{dt} \geq -(\beta_H(t)I_M + \mu_H) \quad (2a)$$

Integrating 2(a) and using the initial conditions, we get

$$S_H(t) \geq -S_{H_0} e^{-(\beta_H(t)I_M + \mu_H)t} > 0 \quad (2b)$$

Again, from second Eq. of (1a), we get

Table 1
Parameter description of the system.

Parameter	Description	Value	Reference
β_M	Transmission rate for mosquitoes	0.3	[27]
δ	Infectious mosquitoes recover	$\frac{1}{30}$	Assumed
$\beta_H(t)$	Time-dependent transmission rate for humans, varying according to the months	$\beta_H(t) = \begin{cases} 0, & 0 \leq t \leq 135 \\ A \sin\left(\frac{2\pi(t-\varphi)}{T}\right), & 135 \leq t \leq 275 \\ 0, & 275 \leq t \leq 360 \end{cases}$	Assumed
α	Exposed individuals become infectious (average duration of the latent period)	$\frac{1}{20}$	[27]
γ	Infectious individuals recover (average duration of the infectious period)	$\frac{1}{30}$	[27]
A	Amplitude (adjust this to control the variation magnitude)	0.3	Assumed
φ	Phase shift (adjust this to control the starting point of the variation)	135	Assumed
T	Period (adjust this to control the length of the seasonal variation)	275	Assumed
μ_H	Natural death rate of human	0.001	Assumed
σ	Death rate of human by the disease	0.001	[28]
Λ_H	Birth rate of human	10^{-6}	Assumed
Λ_M	Birth rate of mosquito	10^{-3}	Assumed
μ_M	Death rate of mosquito	10^{-5}	Assumed

$$\frac{dE_H}{dt} \geq -\alpha E_H - \mu_H E_H \Rightarrow \frac{1}{E_H} \frac{dE_H}{dt} \geq -(\alpha + \mu_H) E_H \quad (2c)$$

Integrating 2(c) and using the initial conditions, we get

$$E_H(t) \geq E_H(0)e^{-(\alpha+\mu_H)t} \geq 0 \quad (2d)$$

Similarly, from third Eq. (1a) to last Eq. (1a), we have

$$\begin{aligned} I_H(t) &\geq I_H(0)e^{-(\gamma+\mu_H+\sigma)t} \geq 0 \\ R_H(t) &\geq R_H(0)e^{-\mu_H t} \geq 0 \\ E_H(t) &\geq E_H(0)e^{-(\alpha+\mu_H)t} \geq 0 \\ S_M(t) &\geq S_M(0)e^{-(\beta_M I_H + \mu_M)t} \geq 0 \\ I_M(t) &\geq I_M(0)e^{-(\delta+\mu_M)t} \geq 0 \\ R_M(t) &\geq R_M(0)e^{-\mu_M t} \geq 0 \end{aligned} \quad (2e)$$

for all t . Therefore, the theorem has been successfully demonstrated and proven.

Theorem 2. All solutions of dynamical system (1a) are uniformly bounded.

Proof: Let, $H = S_H + E_H + I_H + R_H$ and $M = S_M + I_M + R_M$, taking derivative of H with respect to t , then we get,

$$\begin{aligned} \frac{dH}{dt} &= \frac{dS_H}{dt} + \frac{dE_H}{dt} + \frac{dI_H}{dt} + \frac{dR_H}{dt} \\ \Rightarrow \frac{dH}{dt} &= \Lambda_H - (S_H + E_H + I_H + R_H)\mu_H - \sigma I_H \\ \Rightarrow \frac{dH}{dt} &\leq \Lambda_H - H\mu_H \\ \Rightarrow \frac{dH}{dt} + H\mu_H &\leq \Lambda_H \\ \Rightarrow \frac{d}{dt}(He^{\mu_H t}) &\leq \Lambda_H e^{\mu_H t} \end{aligned} \quad (3a)$$

Integrating both sides with respect to t , we get,

$$He^{\mu_H t} \leq \frac{\Lambda_H}{\mu_H} e^{\mu_H t} + \text{constant} \quad (3b)$$

Putting the initial condition $H(0) = (S_{H_0}, E_{H_0}, I_{H_0}, R_{H_0})$, then we get,

$$H \leq \frac{\Lambda_H}{\mu_H} + \left(H(S_{H_0}, E_{H_0}, I_{H_0}, R_{H_0}) - \frac{\Lambda_H}{\mu_H} \right) e^{-\mu_H t} \quad (3c)$$

As t goes to infinity, the above equation changes to

$$\begin{aligned} H &\leq \frac{\Lambda_H}{\mu_H} + H(S_{H_0}, E_{H_0}, I_{H_0}, R_{H_0}) - \frac{\Lambda_H}{\mu_H} \\ H(S_H, E_H, I_H, R_H) &\leq H(S_{H_0}, E_{H_0}, I_{H_0}, R_{H_0}) \end{aligned} \quad (3d)$$

Again, derivative of M with respect to t gives

$$\begin{aligned} \frac{dM}{dt} &= \frac{dS_M}{dt} + \frac{dI_M}{dt} + \frac{dR_M}{dt} \\ \Rightarrow \frac{dM}{dt} &= \Lambda_M - (S_M + I_M + R_M)\mu_M \\ \Rightarrow \frac{dM}{dt} &= \Lambda_M - M\mu_M \\ \Rightarrow \frac{dM}{dt} + M\mu_M &= \Lambda_M \end{aligned} \quad (3e)$$

Using the similar arguments as used for $H(S_H, E_H, I_H, R_H)$, we obtain,

$$M(S_M, I_M, R_M) \leq M(S_{M_0}, I_{M_0}, R_{M_0}) \quad (3f)$$

Therefore, we get,

$$H(S_H, E_H, I_H, R_H) + M(S_M, I_M, R_M) = V \quad (3g)$$

where

$$V \leq H(S_{H_0}, E_{H_0}, I_{H_0}, R_{H_0}) + M(S_{M_0}, I_{M_0}, R_{M_0}) \quad (3h)$$

Hence, all solutions of the system are uniformly bounded.

5. Stability analysis

In this section, the disease-free and endemic equilibria of the proposed model are determined, and the basic reproduction number, R_0 , is calculated using the disease-free equilibrium.

5.1. Disease-free equilibrium (DFE)

The disease-free equilibrium (DFE) in system (1a) is attained by setting all components of the model to zero. Additionally, there are no

instances of infection or recovery at the DFE. Therefore, the DFE in Dengue model (1a) is characterized by

$$\mathcal{D}_{\mathcal{E}} = (S_H^0, E_H^0, I_H^0, R_H^0, S_M^0, I_M^0, R_M^0) \quad (4a)$$

Solving the following equations, we get

$$\left. \begin{array}{l} \Lambda_H - \mu_H S_H^0 = 0 \\ \Lambda_M - \mu_M S_M^0 = 0 \end{array} \right\} \quad (4b)$$

So,

$$S_H^0 = \frac{\Lambda_H}{\mu_H}, S_M^0 = \frac{\Lambda_M}{\mu_M} \quad (4c)$$

Thus, the DFE of proposed model is

$$(S_H^0, E_H^0, I_H^0, R_H^0, S_M^0, I_M^0, R_M^0) = \left(\frac{\Lambda_H}{\mu_H}, 0, 0, 0, \frac{\Lambda_M}{\mu_M}, 0, 0 \right) \quad (4d)$$

5.2. Endemic equilibrium (EE)

The endemic equilibrium (EE) of the dynamical system (1a) is

$$E_E = (S_H^*, E_H^*, I_H^*, R_H^*, S_M^*, I_M^*, R_M^*) \quad (5a)$$

Let's set

$$\frac{dS_H}{dt} = \frac{dE_H}{dt} = \frac{dI_H}{dt} = \frac{dR_H}{dt} = \frac{dS_M}{dt} = \frac{dI_M}{dt} = \frac{dR_M}{dt} = 0 \quad (5b)$$

Then we have

$$\begin{aligned} -\beta_H(t)S_H^*I_M^* + \Lambda_H - \mu_H S_H^* &= 0 \\ \beta_H(t)S_H^*I_M^* - K_2 E_H^* &= 0 \\ \alpha E_H^* - K_3 I_H^* &= 0 \\ \gamma I_H^* - \mu_H R_H^* &= 0 \\ -\beta_M S_M^* I_H^* + \Lambda_M - \mu_M S_M^* &= 0 \\ \beta_M S_M^* I_H^* - K_1 I_M^* &= 0 \\ \delta I_M^* - \mu_M R_M^* &= 0 \end{aligned} \quad (5c)$$

where

$$K_1 = \delta + \mu_M, K_2 = \alpha + \mu_H, K_3 = \gamma + \mu_H + \sigma$$

Solving these equation gives

$$\begin{aligned} I_H^* &= \frac{\alpha}{K_3} E_H^* = A_1 E_H^* \\ R_H^* &= \frac{\alpha \gamma}{\mu_H K_3} \\ E_H^* &= A_2 E_H^* \\ S_M^* &= \frac{\Lambda_M}{\beta_M I_H^* + \mu_M} = \frac{\Lambda_M}{\beta_M A_1 E_H^* + \mu_M} \\ I_M^* &= \frac{1}{K_1} \left[\frac{\beta_M \Lambda_M A_1 E_H^*}{\mu_M + \beta_M A_1 E_H^*} \right] \\ R_M^* &= \frac{\delta}{K_1 \mu_M} \left[\frac{\beta_M \Lambda_M A_1 E_H^*}{\mu_M + \beta_M A_1 E_H^*} \right] \\ S_H^* &= \frac{\Lambda_H}{\beta_H(t) I_M^* + \mu_H} = \frac{\Lambda_H K_1 (\mu_M + \beta_M A_1 E_H^*)}{\beta_H(t) \beta_M \Lambda_M A_1 E_H^* + K_1 \mu_H (\mu_M + \beta_M A_1 E_H^*)} \end{aligned} \quad (5e)$$

From second equation of (5c), we get,

$$E_H^* = 0, E_H^* = \frac{\beta_H(t) \beta_M \Lambda_H \Lambda_M - K_2 \mu_M}{\beta_H(t) \beta_M A_1 K_2 \Lambda_M - K_1 K_2 A_1 \beta_M \mu_M} \quad (5f)$$

However, $E_H^* = 0$ is not feasible once the disease has begun.

Thus, the endemic equilibrium of proposed model is $E_E = (S_H^*, E_H^*, I_H^*, R_H^*, S_M^*, I_M^*, R_M^*)$, where

$$S_H^* = \frac{\Lambda_H K_1 (\mu_M + \beta_M A_1 E_H^*)}{\beta_H(t) \beta_M \Lambda_M A_1 E_H^* + K_1 \mu_H (\mu_M + \beta_M A_1 E_H^*)} \quad (6a)$$

$$E_H^* = \frac{\beta_H(t) \beta_M \Lambda_H \Lambda_M - K_2 \mu_M}{\beta_H(t) \beta_M A_1 K_2 \Lambda_M - K_1 K_2 A_1 \beta_M \mu_M} \quad (6b)$$

$$I_H^* = A_1 E_H^*, R_H^* = A_2 E_H^* \quad (6c)$$

$$S_M^* = \frac{\Lambda_M}{\beta_M A_1 E_H^* + \mu_M}, I_M^* = \frac{1}{K_1} \left[\frac{\beta_M \Lambda_M A_1 E_H^*}{\mu_M + \beta_M A_1 E_H^*} \right], R_M^* = \frac{\delta}{K_1 \mu_M} \left[\frac{\beta_M \Lambda_M A_1 E_H^*}{\mu_M + \beta_M A_1 E_H^*} \right] \quad (6d)$$

with

$$A_1 = \frac{\alpha}{K_3}, A_2 = \frac{\alpha \gamma}{\mu_H K_3}, K_1 = \delta + \mu_M, K_2 = \alpha + \mu_H, K_3 = \gamma + \mu_H + \sigma \quad (6e)$$

5.3. Reproduction number for DFE

In this section, the next-generation matrix method is employed to calculate the basic reproduction number R_0 , which takes into account the F and V matrices [30–32]. These matrices are defined to describe the emergence of new infections and the movement of individuals within compartments other than infectious ones, respectively.

$$\mathcal{F} = \begin{pmatrix} \beta_H(t) S_H I_M \\ 0 \\ \beta_M S_M I_H \end{pmatrix} \quad (7a)$$

$$\mathcal{V} = \begin{pmatrix} (\alpha + \mu_H) E_H \\ -\alpha E_H + (\gamma + \mu_H + \sigma) I_H \\ (\delta + \mu_M) I_M \end{pmatrix} \quad (7b)$$

The Jacobian matrix of f and v at DFE point are as follows:

$$f = \begin{pmatrix} 0 & 0 & \beta_H S_H \\ 0 & 0 & 0 \\ 0 & \beta_M S_M & 0 \end{pmatrix} \quad (7c)$$

$$v = \begin{pmatrix} \alpha + \mu_H & 0 & 0 \\ -\alpha & \gamma + \mu_H + \sigma & 0 \\ 0 & 0 & \delta + \mu_M \end{pmatrix} \quad (7d)$$

Now, the inverse matrix of v is

$$v^{-1} = \begin{pmatrix} \frac{1}{\alpha + \mu_H} & 0 & 0 \\ \frac{\alpha(\delta + \mu_M)}{(\alpha + \mu_H)(\gamma + \mu_H + \sigma)(\delta + \mu_M)} & \frac{1}{\gamma + \mu_H + \sigma} & 0 \\ 0 & 0 & \frac{1}{\delta + \mu_M} \end{pmatrix} \quad (7e)$$

The next generation matrix is

$$fv^{-1} = \begin{pmatrix} 0 & 0 & \frac{\beta_H S_H}{\delta + \mu_M} \\ 0 & 0 & 0 \\ \frac{\alpha(\delta + \mu_M) \beta_M S_M}{(\alpha + \mu_H)(\gamma + \mu_H)(\delta + \mu_M)} & \frac{\beta_M S_M}{\gamma + \mu_H} & 0 \end{pmatrix} \quad (7f)$$

Eigenvalues of fv^{-1} are

$$\begin{aligned} \lambda_1 &= 0 \\ \lambda_2 &= -\frac{1}{(\alpha + \mu_H)} \sqrt{\frac{\beta_H S_H \beta_M S_M (\alpha^2 + \alpha \mu_H)}{(\gamma + \mu_H + \sigma)(\delta + \mu_M)}} \\ \lambda_3 &= \frac{1}{(\alpha + \mu_H)} \sqrt{\frac{\beta_H S_H \beta_M S_M (\alpha^2 + \alpha \mu_H)}{(\gamma + \mu_H + \sigma)(\delta + \mu_M)}} \end{aligned} \quad (7g)$$

Hence, the spectral radius of the $f\nu^{-1}$ i.e., the maximum eigenvalues of $f\nu^{-1}$ is

$$R_0 = \frac{1}{(\alpha + \mu_H)} \sqrt{\frac{\beta_H \beta_M (\alpha^2 + \alpha \mu_H)}{(\gamma + \mu_H + \sigma)(\delta + \mu_M)}} \quad (7h)$$

5.4. Local stability of disease-free equilibrium (\mathcal{D}_E)

Theorem 3. The disease-free equilibrium of system (1a) is locally asymptotically stable for $R_0 < 1$ and unstable for $R_0 > 1$.

Proof: The Jacobian matrix of the model (1a) at DFE point

$$\mathcal{J}_{\mathcal{D}_E} = \begin{pmatrix} \frac{\Lambda_H}{\mu_H}, 0, 0, 0, \frac{\Lambda_M}{\mu_M}, 0, 0 \end{pmatrix}$$

$$J(\mathcal{D}_E) = \begin{bmatrix} -\mu_H & 0 & 0 & 0 & 0 & \frac{\beta_H \Lambda_H}{\mu_H} & 0 \\ 0 & -(\alpha + \mu_H) & 0 & 0 & 0 & \frac{\beta_H \Lambda_H}{\mu_H} & 0 \\ 0 & \alpha & -(\gamma + \mu_H + \sigma) & 0 & 0 & 0 & 0 \\ 0 & 0 & \gamma & -\mu_H & 0 & 0 & 0 \\ 0 & 0 & \frac{\beta_M \Lambda_M}{\mu_M} & 0 & -\mu_M & 0 & 0 \\ 0 & 0 & \frac{\beta_M \Lambda_M}{\mu_M} & 0 & 0 & -(\delta + \mu_M) & 0 \\ 0 & 0 & 0 & 0 & 0 & \delta & -\mu_M \end{bmatrix} \quad (8a)$$

Now,

$$|J(\mathcal{D}_E) - \lambda I| = \begin{vmatrix} -\mu_H - \lambda & 0 & 0 & 0 & 0 & \frac{\beta_H \Lambda_H}{\mu_H} & 0 \\ 0 & -(\alpha + \mu_H + \lambda) & 0 & 0 & 0 & \frac{\beta_H \Lambda_H}{\mu_H} & 0 \\ 0 & \alpha & -(\gamma + \mu_H + \sigma + \lambda) & 0 & 0 & 0 & 0 \\ 0 & 0 & \gamma & -\mu_H - \lambda & 0 & 0 & 0 \\ 0 & 0 & \frac{\beta_M \Lambda_M}{\mu_M} & 0 & -\mu_M - \lambda & 0 & 0 \\ 0 & 0 & \frac{\beta_M \Lambda_M}{\mu_M} & 0 & 0 & -(\delta + \mu_M + \lambda) & 0 \\ 0 & 0 & 0 & 0 & 0 & \delta & -\mu_M - \lambda \end{vmatrix}$$

The characteristic equation is

$$|J(\mathcal{D}_E) - \lambda I| = 0$$

$$-(\mu_H + \lambda) * \begin{vmatrix} -(\alpha + \mu_H + \lambda) & 0 & 0 & 0 & \frac{\beta_H \Lambda_H}{\mu_H} & 0 \\ \alpha & -(\gamma + \mu_H + \sigma + \lambda) & 0 & 0 & 0 & 0 \\ 0 & \gamma & -(\mu_H + \lambda) & 0 & 0 & 0 \\ 0 & \frac{\beta_M \Lambda_M}{\mu_M} & 0 & -(\mu_M + \lambda) & 0 & 0 \\ 0 & \frac{\beta_M \Lambda_M}{\mu_M} & 0 & 0 & -(\delta + \mu_M + \lambda) & 0 \\ 0 & 0 & 0 & 0 & \delta & -(\mu_M + \lambda) \end{vmatrix} = 0$$

$$(\mu_H + \lambda) * (\mu_M + \lambda) * \begin{vmatrix} -(\alpha + \mu_H + \lambda) & 0 & 0 & 0 & \frac{\beta_H \Lambda_H}{\mu_H} & 0 \\ \alpha & -(\gamma + \mu_H + \sigma + \lambda) & 0 & 0 & 0 & 0 \\ 0 & \gamma & -(\mu_H + \lambda) & 0 & 0 & 0 \\ 0 & \frac{\beta_M \Lambda_M}{\mu_M} & 0 & -(\mu_M + \lambda) & 0 & 0 \\ 0 & \frac{\beta_M \Lambda_M}{\mu_M} & 0 & 0 & -(\delta + \mu_M + \lambda) & 0 \end{vmatrix} = 0$$

$$\begin{aligned}
& (\mu_H + \lambda) * (\mu_M + \lambda) * (\mu_H + \lambda) * (\mu_M + \lambda) \\
& * \begin{vmatrix} -(\alpha + \mu_H + \lambda) & 0 & \frac{\beta_H \Lambda_H}{\mu_H} \\ \alpha & -(\gamma + \mu_H + \sigma + \lambda) & 0 \\ 0 & \frac{\beta_M \Lambda_M}{\mu_M} & -(\delta + \mu_M + \lambda) \end{vmatrix} = 0 \\
& (\mu_H + \lambda) * (\mu_M + \lambda) * (\mu_H + \lambda) * (\mu_M + \lambda) \\
& * \left[(\alpha + \mu_H + \lambda)(\gamma + \mu_H + \sigma + \lambda)(\delta + \mu_M + \lambda) - \alpha * \frac{\beta_H \Lambda_H}{\mu_H} * \frac{\beta_M \Lambda_M}{\mu_M} \right] = 0
\end{aligned}$$

Assume that

$$B_1 = (\alpha + \mu_H), B_2 = (\gamma + \mu_H + \sigma), B_3 = (\delta + \mu_M), B_4 = \alpha * \frac{\beta_H \Lambda_H}{\mu_H} * \frac{\beta_M \Lambda_M}{\mu_M} \quad (8b)$$

We have found four eigenvalues all are negative. The rest will be obtained by the Routh- Hurwitz [33] criteria based on the following polynomial

$$(B_1 + \lambda)(B_2 + \lambda)(B_3 + \lambda) - B_4 = 0 \quad (8c)$$

After simplification, we get the cubic polynomial,

$$\lambda^3 + B_5 \lambda^2 + B_6 \lambda + B_7 = 0 \quad (8d)$$

where

$$B_5 = (B_1 + B_2 + B_3), B_6 = (B_1 B_2 + B_2 B_3 + B_3 B_1), B_7 = B_1 B_2 B_3 - B_4 \quad (8e)$$

All coefficient of the polynomial i.e., B_5 and B_6 are positive and B_7 is positive based on the following condition $B_1 B_2 B_3 > B_4$. Finally, we found all eigenvalues are strictly negative. According to the Ruth- Hurwitz criteria we have proven that the theorem is locally asymptotically stable for $R_0 < 1$. When the condition $B_1 B_2 B_3 > B_4$ disagreed, the system will be unstable means $R_0 > 1$, the diseases Dengue will be in active face and it persists. Hence the theorem.

5.5. Global stability of disease-free equilibrium (\mathcal{D}_E)

Let us consider the feasible region $\omega_1 = \{X \in \omega : S_H \leq S_H^0, S_M \leq S_M^0\}$, where $X = \{S_H, E_H, I_H, R_H, S_M, I_M, R_M\}$ and to show that ω_1 is invariant under the following lemma.

Lemma 1. *The region ω_1 is a positively invariant for the proposed Dengue model (1a).*

Proof: From the first equation of the model (1a), we have

$$\frac{dS_H}{dt} = \Lambda_H - \beta_H S_H I_M - \mu_H S_H \leq \Lambda_H - \mu_H S_H \leq \mu_H \left(\frac{\Lambda_H}{\mu_H} - S_H \right) \leq \mu_H (S_H^0 - S_H) \quad (9a)$$

which gives,

$$S_H \leq S_H^0 - (S_H^0 - S_H(0)) e^{-\mu_H t} \quad (9b)$$

Thus if $S_H(0) \leq S_H^0$ for all $t \geq 0$, then $S_H(t) \leq S_H^0$ for all $t \geq 0$. From the fifth equation of the Dengue model (1a) we have,

$$\begin{aligned}
\frac{dS_M}{dt} &= \Lambda_M - \beta_M S_M I_H - \mu_M S_M \leq \Lambda_M - \mu_M S_M \leq \mu_M \left(\frac{\Lambda_M}{\mu_M} - S_M \right) \\
&\leq \mu_M (S_M^0 - S_M)
\end{aligned} \quad (9c)$$

which gives,

$$S_M \leq S_M^0 - (S_M^0 - S_M(0)) e^{-\mu_M t} \quad (9d)$$

Thus if $S_M(0) \leq S_M^0$ for all $t \geq 0$, then $S_M(t) \leq S_M^0$ for all $t \geq 0$.

By summing the above two equations, it can be deduced that region ω_1 is positively invariant and attracts all solutions in R_+^7 for the Dengue model (1a). In the following theorem, we delve into the global asymptotic stability of DFE point \mathcal{D}_E .

Theorem 4. *If the vector-host mathematical model can be written in general form as*

$$\frac{dX_1}{dt} = F(X_1, X_2), \frac{dX_2}{dt} = G(X_1, X_2), G(X_1, 0) = 0 \quad (10a)$$

where, $X_1 = (S_H, R_H, S_M, R_M)^t$, and $X_2 = (E_H, I_H, I_M)^t$ represent the infected and uninfected individuals, then the disease-free equilibrium point is globally asymptotically stable for $R_0 < 1$.

Proof: The DFE is now represented here by

$$E_0 = (X_1^0, 0) = \left(\frac{\Lambda_H}{\mu_H}, 0, 0, 0, \frac{\Lambda_M}{\mu_M}, 0, 0 \right) \quad (10b)$$

For the global asymptomatic stability of E_0 , the condition H_1 and H_2 given below must be satisfied.

$H_1 : \frac{dx_1}{dt} = F(X_1^0, 0), X_1^0$ is global asymptomatic stable, $H_2 : \hat{G}(X_1, X_2) = AX_2 - G(X_1, X_2), \hat{G}(X_1, X_2) \geq 0$, where $A = D_{X_2} F(X_1^0, 0)$ is a Metzler matrix? If the (1a) satisfied Eq. (6) then the equilibrium point $\mathcal{D}_E = (X_1^0, 0)$ is a global asymptomatic stable equilibrium provided $R_0 < 1$.

A different way to address the similar theoretical issue is discussed at Theorem 5

Theorem 5. *The equilibrium point $\mathcal{D}_E = (X_1^0, 0)$ is a global asymptomatic stable equilibrium provided $R_0 < 1$ and the conditions of equation (6) satisfies.*

Proof: By applying theorem 3 to a mathematical model (1a), we consider

$$F(X_1^0, 0) = \Lambda_H - \mu_H S_H, \hat{G}(X_1, X_2) = AX_2 - G(X_1, X_2) \quad (11a)$$

where

$$A = \begin{bmatrix} -(\alpha + \mu_H) & 0 & \beta_H S_H^0 \\ \alpha & -(\gamma + \sigma + \mu_H) & 0 \\ 0 & \beta_M S_M^0 & -(\delta + \mu_M) \end{bmatrix} \quad (11b)$$

Now,

$$\hat{G}(X_1, X_2) = AX_2 - G(X_1, X_2)$$

$$= \begin{bmatrix} -(\alpha + \mu_H)E_H + \beta_H S_H^0 I_M \\ \alpha E_H - (\gamma + \sigma + \mu_H)I_H \\ \beta_M S_M^0 I_H - (\delta + \mu_M)I_M \end{bmatrix} - \begin{bmatrix} \beta_H S_H I_M - \alpha E_H - \mu_H E_H \\ \alpha E_H - \gamma I_H - \sigma I_H - \mu_H I_H \\ \beta_M S_M I_H - \delta I_M - \mu_M I_M \end{bmatrix} \quad (11c)$$

$$= \begin{bmatrix} \beta_H I_M (S_H^0 - S_H) \\ 0 \\ \beta_M I_H (S_M^0 - S_M) \end{bmatrix} = \begin{bmatrix} \hat{G}_1 \\ \hat{G}_2 \\ \hat{G}_3 \end{bmatrix} \quad (11d)$$

Clearly, $\hat{G}_1 \geq 0$, $\hat{G}_2 = 0$ and $\hat{G}_3 \geq 0$, since $S_H \leq S_H^0, S_M \leq S_M^0$. Therefore,

$$\hat{G}(X_1, X_2) \geq 0 \quad (11e)$$

Also, by the definition of Metzler matrix we can say that the matrix A is similar to Metzler matrix.

Hence, DFE (\mathcal{D}_E) is global asymptotically stable [34].

5.6. Global stability of endemic equilibrium (E_E)

Theorem 6. If $R_0 > 1$, the endemic equilibrium (E_E) is globally asymptotically stable.

Proof: We take into consideration the form's Lyapunov function

$$W(t) = \frac{1}{2}(S_H - S_H^*)^2 + \frac{1}{2}(E_H - E_H^*)^2 + \frac{1}{2}(I_H - I_H^*)^2 + \frac{1}{2}(R_H - R_H^*)^2 + \frac{1}{2}(S_M - S_M^*)^2 + \frac{1}{2}(I_M - I_M^*)^2 + \frac{1}{2}(R_M - R_M^*)^2 \quad (12a)$$

Differentiating the above equation with respect to t , we get,

$$W'(t) = (S_H - S_H^*)(S'_H) + (E_H - E_H^*)(E'_H) + (I_H - I_H^*)(I'_H) + (R_H - R_H^*)(R'_H) + (S_M - S_M^*)(S'_M) + (I_M - I_M^*)(I'_M) + (R_M - R_M^*)(R'_M) \quad (12b)$$

$$\begin{aligned} &= (S_H - S_H^*)(-\beta_H(t)S_H I_M + \Lambda_H - \mu_H S_H) + (E_H - E_H^*)(\beta_H(t)S_H I_M - \alpha E_H \\ &\quad - \mu_H E_H) + (I_H - I_H^*)(\alpha E_H - \gamma I_H - \mu_H I_H - \sigma I_H) + (R_H - R_H^*)(\gamma I_H \\ &\quad - \mu_H R_H) + (S_M - S_M^*)(-\beta_M S_M I_H + \Lambda_M - \mu_M S_M) + (I_M - I_M^*)(\beta_M S_M I_H \\ &\quad - \delta I_M - \mu_M I_M) + (R_H - R_H^*)(\delta I_M - \mu_M R_M) \end{aligned} \quad (12c)$$

Using the equilibrium conditions

$$\Lambda_H = \mu_H S_H^* + \mu_H E_H^* + \mu_H I_H^* + \mu_H R_H^* - \sigma I_H^* \quad (12d)$$

and

$$\Lambda_M = \mu_M S_M^* + \mu_M I_M^* + \mu_M R_M^* \quad (12e)$$

into the above equation

$$\begin{aligned} W'(t) &= (S_H - S_H^*)(-\beta_H(t)S_H I_M + \mu_H S_H^* + \mu_H E_H^* + \mu_H I_H^* + \mu_H R_H^* - \sigma I_H^* \\ &\quad - \mu_H S_H) + (E_H - E_H^*)(\beta_H(t)S_H I_M - \alpha E_H - \mu_H E_H) + (I_H - I_H^*)(\alpha E_H - \gamma I_H - \mu_H I_H \\ &\quad - \sigma I_H) + (R_H - R_H^*)(\gamma I_H - \mu_H R_H) + (S_M - S_M^*)(-\beta_M S_M I_H \\ &\quad - \beta_M S_M I_H + \mu_M S_M^* + \mu_M I_M^* + \mu_M R_M^* - \mu_M S_M) + (I_M - I_M^*)(\beta_M S_M I_H - \delta I_M \\ &\quad - \mu_M I_M) + (R_H - R_H^*)(\delta I_M - \mu_M R_M) \end{aligned} \quad (12f)$$

$$\begin{aligned} W'(t) &= -\mu_H(S_H - S_H^*)^2 - \beta_H(S_H - S_H^*)S_H I_M + \mu_H E_H^*(S_H - S_H^*) \\ &\quad + (\mu_H - \sigma)(S_H - S_H^*)I_H^* + \mu_H(S_H - S_H^*)R_H^* + \beta_H(t)S_H I_M(E_H - E_H^*) \\ &\quad - (\mu_H + \alpha)(E_H - E_H^*) + \alpha E_H(I_H - I_H^*) - (\gamma + \sigma + \mu_H)(I_H - I_H^*)I_H \\ &\quad + \gamma(R_H - R_H^*)I_H - \mu_H(R_H - R_H^*)R_H - \beta_M S_M I_H(S_M - S_M^*) \\ &\quad + \mu_M(S_M - S_M^*)^2 + \mu_M I_M^*(S_M - S_M^*) + \mu_M R_M^*(S_M - S_M^*) \\ &\quad + \beta_M S_M I_H(I_M - I_M^*) - (\delta + \mu_M)(I_M - I_M^*) + \delta I_M(R_H - R_H^*) \\ &\quad - \mu_M R_M(R_H - R_H^*) \end{aligned} \quad (12g)$$

Since,

$$S_H \leq S_H^*, E_H \leq E_H^*, I_H \leq I_H^*, R_H \leq R_H^*, S_M \leq S_M^*, I_M \leq I_M^*, R_M \leq R_M^* \quad (12h)$$

So, the above equation shows that $W'(t) \leq 0$ and $W'(t) = 0$ for

$$S_H = S_H^*, E_H = E_H^*, I_H = I_H^*, R_H = R_H^*, S_M = S_M^*, I_M = I_M^*, R_M = R_M^* \quad (12i)$$

Thus, the singleton set E_E is the largest invariance set. As a result of LaSalle's invariance [35], the endemic equilibrium E_E is globally asymptotically stable.

6. Sensitivity analysis

Sensitivity analysis identifies the factors with the most significant impact on R_0 in the proposed dynamical system. This information can assist public health officials in prioritizing their efforts to prevent and control the spread of the Dengue virus. The normalized forward sensitivity index quantifies the sensitivity of R_0 to changes in specific pa-

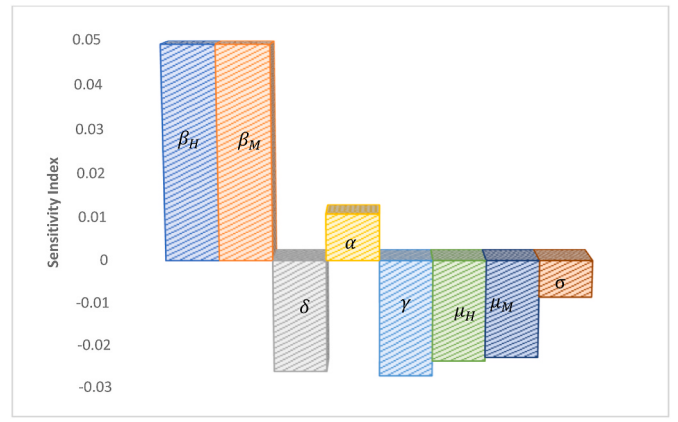


Fig. 2. Impact of model parameters on R_0 .

rameters, and this metric is applied to model (1a), denoted by,

$$\Gamma_{R_0}^\sigma = \frac{\sigma}{R_0} \frac{\partial R_0}{\partial \sigma} \quad (13)$$

where the higher sensitivity index influences the basic reproduction number (R_0). Furthermore, it spreads the disease increasingly. As the disease transmission rate for humans is time-dependent, the sensitivity analysis for such a variable has more impact on the transmission Fig. 2. The rest of the parameters are explicitly obtained, but the time-dependent transmission rate for humans has two different aspects. Due to proposed dynamical sectional continuous functions, its derivative can be expressed either based on exponential function for a certain time when Dengue is in action, or it might be neglected in the rest period because of its null appearance.

$$\Gamma_{R_0}^\alpha = \frac{\alpha}{R_0} \frac{\partial R_0}{\partial \alpha} = \frac{\mu_H \sqrt{\alpha}}{2(\alpha + \mu_H)}, \Gamma_{R_0}^\delta = \frac{\delta}{R_0} \frac{\partial R_0}{\partial \delta} = -\frac{\delta}{2(\delta + \mu_H)}$$

$$\Gamma_{R_0}^{\mu_M} = \frac{\mu_M}{R_0} \frac{\partial R_0}{\partial \mu_M} = -\frac{\mu_M}{2(\delta + \mu_M)}, \Gamma_{R_0}^\gamma = \frac{\gamma}{R_0} \frac{\partial R_0}{\partial \gamma} = -\frac{\gamma}{2(\gamma + \mu_H + \sigma)}$$

$$\Gamma_{R_0}^\sigma = \frac{\sigma}{R_0} \frac{\partial R_0}{\partial \sigma} = -\frac{\sigma}{2(\gamma + \mu_H + \sigma)}, \Gamma_{R_0}^{\beta_M} = \frac{\beta_M}{R_0} \frac{\partial R_0}{\partial \beta_M} = \frac{1}{2}$$

$$\Gamma_{R_0}^{\beta_H} = \frac{\beta_H}{R_0} \frac{\partial R_0}{\partial \beta_H(t)} = \frac{1}{2} \frac{2A\pi \cos \frac{2\pi(t-\varphi)}{T}}{T} = \frac{A\pi}{T} \left[e^{\frac{2\pi i(t-\varphi)}{T}} + e^{-\frac{2\pi i(t-\varphi)}{T}} \right]$$

The $\Gamma_{R_0}^{\beta_H}$ is valid for the range described in Table 1. The rest of the time of the year is 0.

The sensitivity analysis of this study found that the recovery rate of infected humans in the host population has the most negative sensitivity index (2.74%) from Table 2 and Fig. 1. It means that a small change in this rate can greatly impact. Other important factors with negative sensitivity indices, for the vector, the small change in the natural death rate of mosquitoes has increased (decreased) the number of infected humans.

On the other hand, the per capita contact rate from mosquitoes to humans (β_H) and humans to mosquitoes (β_M) has positive sensitivity indices. It means that a small increase in this rate can also greatly impact

Table 2
Sensitivity indices of R_0 .

Parameter	Sensitivity Index	Parameter	Sensitivity Index
β_H	+ 0.0488	γ	- 0.0274
β_M	+ 0.0488	μ_H	- 0.0238
δ	- 0.0263	μ_M	- 0.0229
α	+ 0.0107	σ	- 0.0085

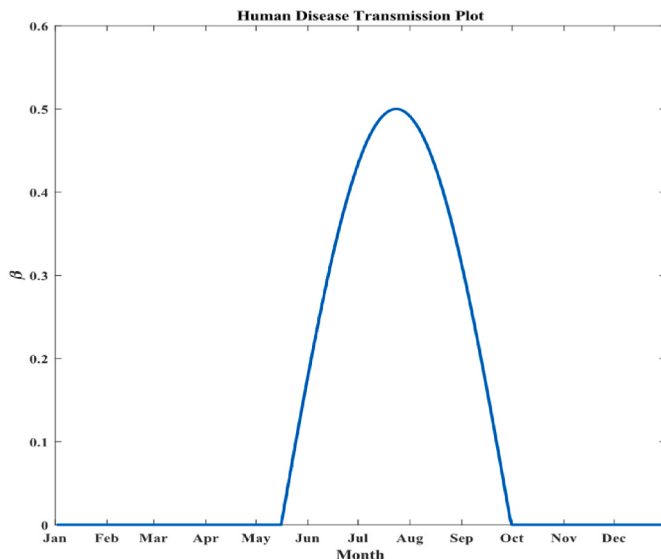


Fig. 3. The disease transmission rate for humans over the year.

disease. In conclusion, this sensitivity analysis provides valuable information about the factors that most influence the spread of Dengue virus. This information can be used to develop effective prevention and control strategies.

7. Results and discussion

The primary objective of the proposed Dengue model is to forecast the future count of infected individuals, aiding the government of Bangladesh in disease prevention measures. These measures may involve augmenting healthcare resources, such as hospitals, beds, doctors, and support staff. Furthermore, city corporations can undertake initiatives to minimize Aedes mosquito larvae, eliminate adult mosquitoes, improve sanitation in stagnant water areas, and enhance the mortality rate of mosquito eggs.

Analyzing Dengue infection data sourced from the Institute of Epidemiology, Disease Control and Research (IDCER) in Bangladesh and World health Organization, we examined data spanning from January 2001 to December 2022 for monthly records and from January 2022 to October 2023 for daily records [36,37]. The results reveal a noteworthy pattern: a significant upsurge in the number of infected individuals during the summer months, starting from mid-May and extending

through October.

This phenomenon coincides with the heightened activity of Aedes mosquitoes. Fig. 3 illustrates this trend, showcasing a consistent increase in disease transmission rates during this period, while transmission rates approach zero during other months. This pattern remains consistent from 2001 to 2023, with one notable exception: in 2019, disease transmission rates remained elevated even into November. This anomaly suggests an unusual mosquito activity pattern during the autumn of 2019.

To further clarify the findings, simulations of the system (1a) were conducted, and the dynamics are illustrated in Fig. 4. This figure conveys a message akin to Fig. 3, highlighting that disease transmission remains dormant from January to Mid-May and from November to December. During these periods, infected mosquitoes can recover without transmitting the infection to humans. Conversely, from Mid-May to October, disease transmission becomes active, facilitating the transmission of infections between humans and Aedes mosquitoes. Upon analyzing government data, it becomes evident that the disease contact rate from mosquitoes to humans remains nearly negligible during the periods from January to Mid-May and November to December.

To gain a more comprehensive understanding, we have dissected the time series into two distinct components: one representing the human population (displayed in the left panel of Fig. 4), and the other representing the mosquito population (illustrated in the right panel of Fig. 4). Regarding humans, it's important to note that initially, 25 % of mosquitoes are infected with the disease. Starting in January, these infected mosquitoes will commence the recovery process, and by Mid-May, the disease will begin to propagate among humans. In addition, the disease peaks between August and September and it falls from the following month.

However, by November, the mosquitoes don't spread disease to humans, but infected humans recovered from disease throughout the following months. For a more detailed examination, the time series has been divided into two components: one representing the human population (left panel of Fig. 4) and the other representing the mosquito population (right panel of Fig. 4).

Fig. 5 displays the time series of infected humans and mosquitoes for varying values of A and β_M . The left panel of Fig. 5 illustrates that the count of infected humans rises with increasing β_M , while the right panel of Fig. 5 demonstrates a corresponding increase in infected mosquitoes as A increases. Notably, Fig. 5 reveals that the duration of the disease outbreak is influenced by the amplitude, A . This observation holds biological significance because augmenting both A and β_M amplifies the density of infected humans and mosquitoes. It's worth noting that the

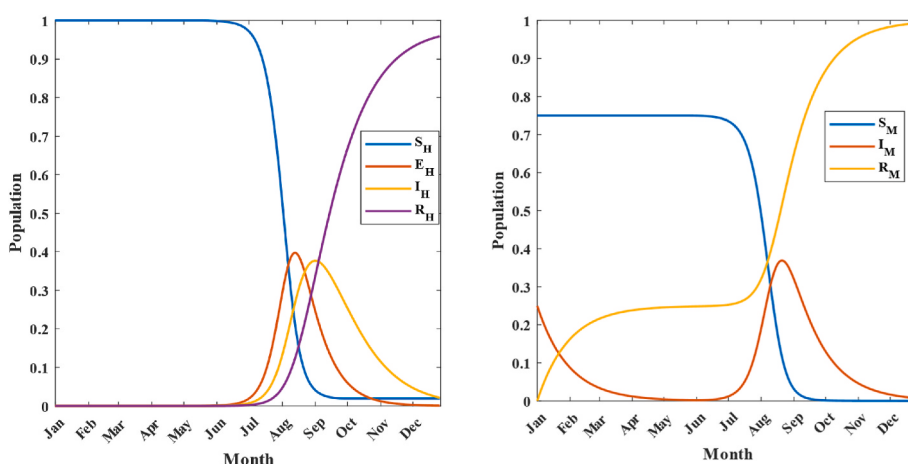


Fig. 4. Time trace of vector incident. Left panel is for human compartments and the right panel is for mosquito compartments. At the start, the initial values are set as follows: $S_M = 0.75, I_M = 0.25, R_M = 0$ for mosquitoes, and $S_H = 1, E_H = 0, I_H = 0, R_H = 0$. The values of the parameters are $\beta_M = 0.3, \delta = 0.0333, \alpha = 0.05, \gamma = 0.0333$.

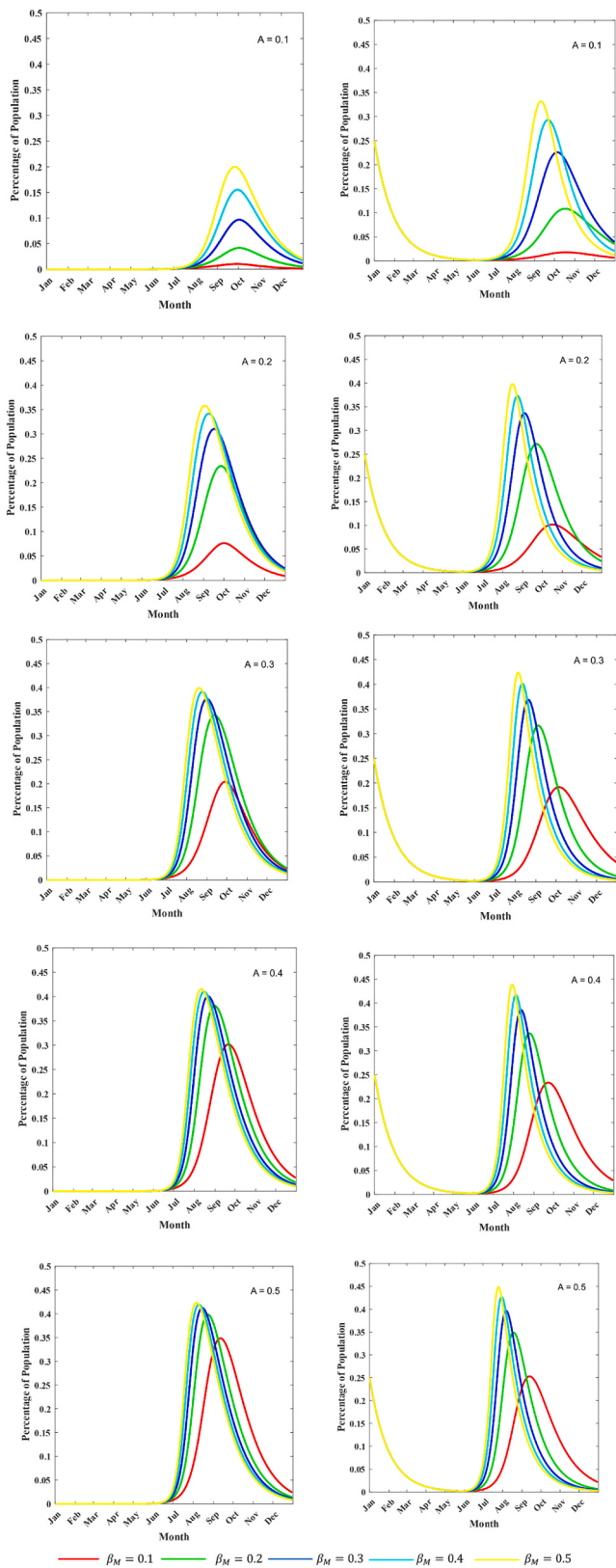


Fig. 5. Time series of Infected populations, humans and mosquitoes for different amplitudes (A), and contact rate of host to vector (β_M).

model's sensitivity is most pronounced in the parameter γ , which can be enhanced through a healthy diet and regular exercise.

Fig. 6 presents a series of 2D graphs showcasing the final epidemic size for both humans and mosquitoes. These graphs are divided into two panels, (a) and (b), each containing two sub-figures, denoted as (i) and (ii). The color scheme utilizes red shading to represent the infected population, while blue indicates the disease-free portion. The graphs illustrate the interplay between three key factors such as mosquito to human disease transmission rate (β_H) that depends on amplitude (A), human to mosquito disease transmission rate (β_M), and human recovery rate (γ).

Sub-figures a (i) and b (i) demonstrate that a disease-free portion exists when either the human transmission rate (amplitude: A) is high, but the mosquito transmission rate (β_M) approaches zero or the mosquito transmission rate (β_M) is high, but the human transmission rate (Amplitude: A) remains below a critical threshold. Conversely, sub-figures a (i) and b (i) depict a scenario where the disease spreads throughout the population when both the human transmission rate exceeds 0.15 and the mosquito transmission rate is greater than 0.2. Similar expressions can be used to revoke the behavior of a (ii) and b (ii).

The Dengue incidence dataset, period from January 1, 2022, to October 8, 2023, shows significant attributes. The main trend is represented by a median of 40 and a mean of 498.59, suggesting a right-skewed distribution due to the higher mean. The standard deviation of 859.84 and a coefficient of variation of 1.725 highlight substantial variability in the data. The positive skewness of 1.771 indicates an asymmetry with a longer right tail, reflecting the presence of higher incidence values. The Shapiro-Wilk test, with a statistic of 0.629 and a p-value less than 0.001, indicates non-normality in the distribution. Additionally, the kurtosis of 1.712 suggests heavier tails than a normal distribution. The dataset's range from a minimum of 0 to a maximum of 3123 and percentiles (25th at 4 and 75th at 482) underscore the broad range of dengue incidence observed. Details are presented in Table 3.

Consequently, Aedes mosquitoes cease to infect humans unless the mosquito contact rate remains high, although humans can still transmit the infection to mosquitoes. It is worth noting that all the 2D graphs in this figure represent the disease-free equilibrium region, depicted in blue.

The infected data, which had been collected from the government of Bangladesh, was subjected to the application of our proposed system (1a). As illustrated in Fig. 7, the infected data generated by the model exhibited an impressive fit to the original infected data, achieving an impressive level of accuracy, estimated at approximately 85 %. We determine the calculation error of our model from the real data in Fig. 8. However, it is essential to note that the accuracy of this prediction is influenced by the model parameters. These model parameters, crucial in determining the model's performance, tend to undergo variations from one year to another Fig. 7.

The model can learn complex patterns and relationships that conventional models may not capture by training on historical Dengue incidence data. Traditional epidemiological models rely on mathematical equations and assumptions about disease transmission dynamics. This data-driven insight allows a more nuanced understanding of the factors influencing Dengue outbreaks. ML approach is inherently adaptable to changing conditions and emerging trends. As Dengue dynamics evolve due to climate change, urbanization, and variations in healthcare infrastructure, the model can seamlessly adjust to these shifts. This adaptability ensures that the predictions remain relevant and reliable in dynamic epidemiological contexts [39].

As discussed in this section, the flowchart in Fig. 9 outlines the sequential steps in machine learning-based dengue epidemic forecasting. It visually represents the stages encompassing historical data collection, preprocessing, model selection, model training, and the subsequent generation of forecasts customized for dengue cases.

To ensure the accuracy and integrity of the dataset, we conducted a thorough manual verification process Table 4. The objective was to

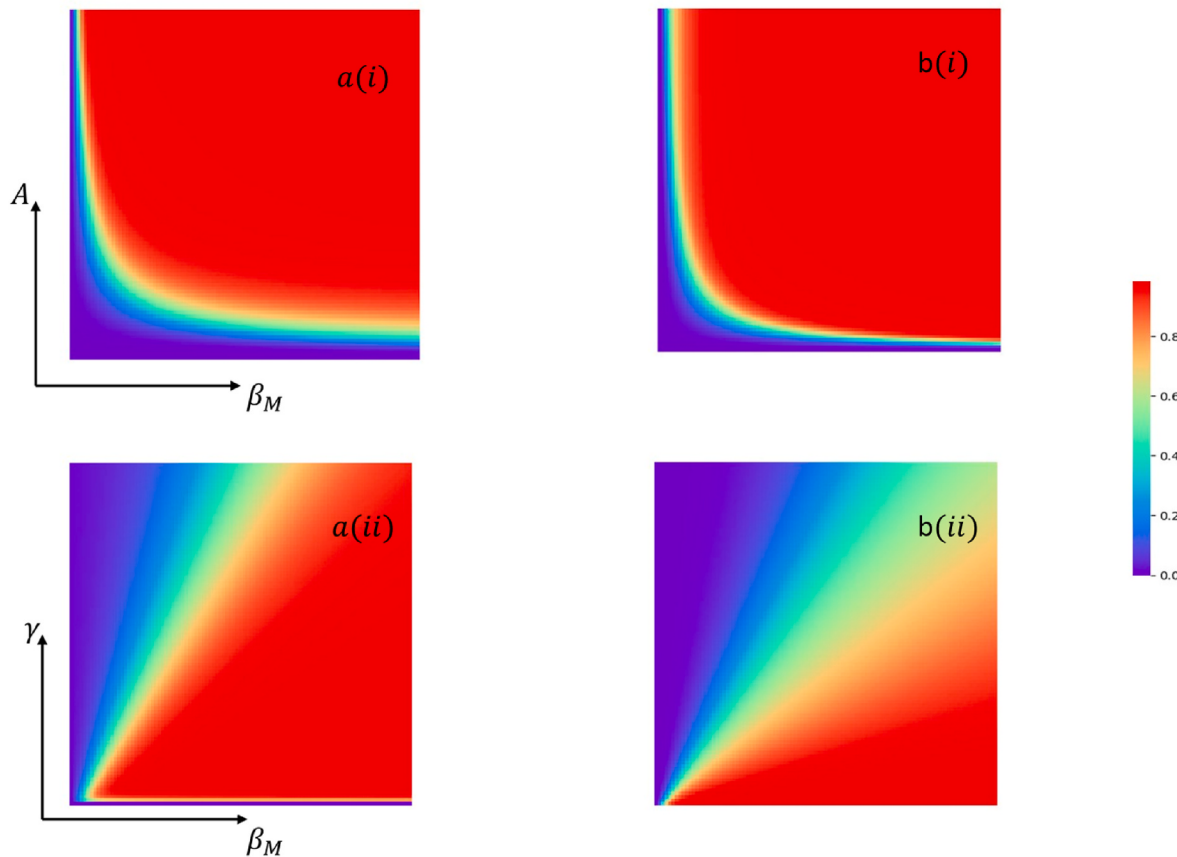


Fig. 6. Two-dimensional phase diagram representing, for (a-*), final epidemic size of human and for (b-*), final epidemic size of mosquito measured in individuals over the amplitude (A), recovery rate (γ), and contact rate of mosquito (β_M).

Table 3
Descriptive data.

	Dengue Incidence
Median	40
Mean	498.59
Std. Error of Mean	33.24
Std. Deviation	859.04
Coefficient of variation	1.725
Skewness	1.771
Std. Error of Skewness	0.094
Kurtosis	1.712
Std. Error of Kurtosis	0.189
Shapiro-Wilk	0.629
p-value of Shapiro-Wilk	< 0.001
Minimum	0
Maximum	3123

confirm the absence of any missing or anomalous values within the dataset. As a product of this verification process, the refined dataset is our model's historical dataset. This dataset forms the foundation for predicting future probabilities. The visualization of the training (historical) data subjected to smoothing through a 7-day moving average in its raw form is depicted in Fig. 10.

These visualizations serve as pivotal tools for comprehending the inherent trends and patterns within the collected data, providing invaluable insights that inform our modeling approach. The visualization shows that the number of dengue cases begins to rise from June to July in Bangladesh, coinciding with the onset of the rainy season, which supports the findings of WHO [38]. The findings also indicate that the dengue rate in Bangladesh starts to increase from June to July due to the monsoon season. The direct correlation between rainwater and the

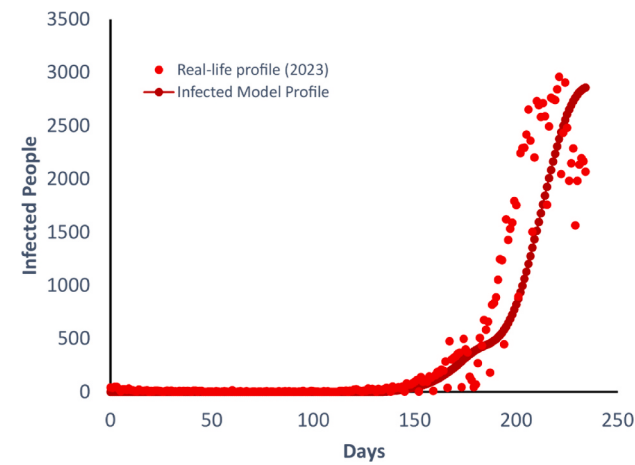


Fig. 7. Comparing Infected Human data and proposed Dengue dynamics.

breeding of Dengue or Aedes mosquitoes [40] becomes apparent during this period. The peak of dengue cases occurs between August and October each year, according to this visualization. Although not exactly similar, it mostly aligns with the findings from (Hossain et al., 2023) [41], where they found that dengue in Bangladesh historically peaked during the monsoon and post-monsoon seasons. Previously, the peak was from August to September, but in recent times, especially from 2022, the peak is also observed in October, and the peak is shifting day by day due to climate change [41]. Furthermore, according to our visualization, a notable decline is observed, from 0 to 100 cases, in November and December, corresponding to the conclusion of the

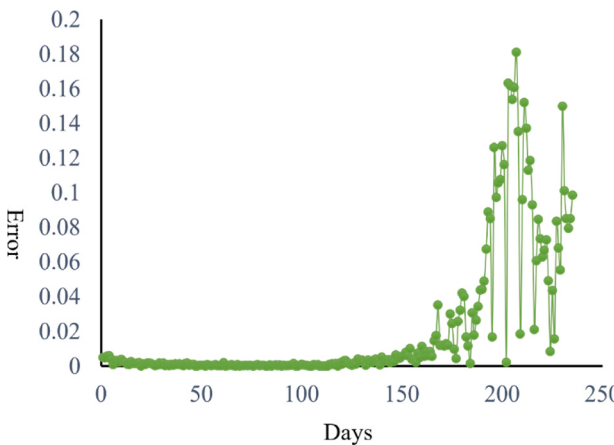


Fig. 8. Error analysis of government-infected data and dynamical model-infected data.

monsoon seasons and the commencement of winter, similar to the findings from (Islam et al., 2021) [42]. They showed a correlation between the rainy season and the dengue outbreak as the major factor for the dengue outbreak and a decrease in the dry winter season of the same year [42].

We detail our approach to model selection for dengue forecasting utilizing Auto-regressive Integrated Moving Average (ARIMA), Long Short-Term Memory (LSTM) networks [43], and Prophet models [43]. Each model is chosen based on its suitability for capturing different aspects of the time series data, ranging from basic statistical methods to advanced deep learning architectures. We divided the available data into training and validation sets in our implementation. We used 90 % of the data from January 1, 2022, to August 4, 2023, for training purposes, while the remaining 10 % from August 5 to October 8, 2023, was allocated for validation. We employed the trained models for forecasting the next 365 days based on this data [45]. Our results are good enough based on the performance selected for analysis. The trained models were subsequently applied to forecast dengue cases for the upcoming year, starting from October 9, 2023. We selected three distinct models for our dengue forecasting task:

- (i) **ARIMA (Autoregressive Integrated Moving Average):** A traditional statistical model for capturing temporal dependencies and trends. It was defined with an order of $(7, 2, 2)$, indicating the autoregressive, differencing, and moving average components. It was then trained on the training set and validation on the validation set. Then, error metrics were calculated based on the validation set.
- (ii) **LSTM (Long Short-Term Memory):** A deep learning model that captures intricate patterns and dependencies in sequential data. The dataset was preprocessed using Min-Max scaling. Both the training and test sets are scaled accordingly. Sequences of length

seven was created from the scaled data. The LSTM model uses Keras with a sequential architecture. It consists of an LSTM layer with 50 neurons and a rectified linear using (ReLU) activation function. The output layer was a dense layer with one neuron. The model was compiled with the RMSProp optimizer and mean squared error (MSE) loss. It was then trained on the training sequences for 100 epochs.

- (iii) **Prophet:** A forecasting tool developed by Facebook [44], specifically designed for time series data with strong seasonal effects and multiple seasons of historical data. Prophet adopts a decomposable time series model (Harvey & Peters 1990) [46] comprising three fundamental components: trend, seasonality, and holidays. The model equation is elegantly expressed as:

$$y(t) = g(t) + s(t) + h(t) + \epsilon_t$$

Where $g(t)$ represents the trend function that adept at capturing non-periodic changes, $s(t)$ captures periodic changes such as weekly and

Table 4
Sample data.

Date	Total Count
2023-08-19	1983
2023-08-20	2134
2023-08-21	2197
2023-08-22	2168
2023-08-23	2070

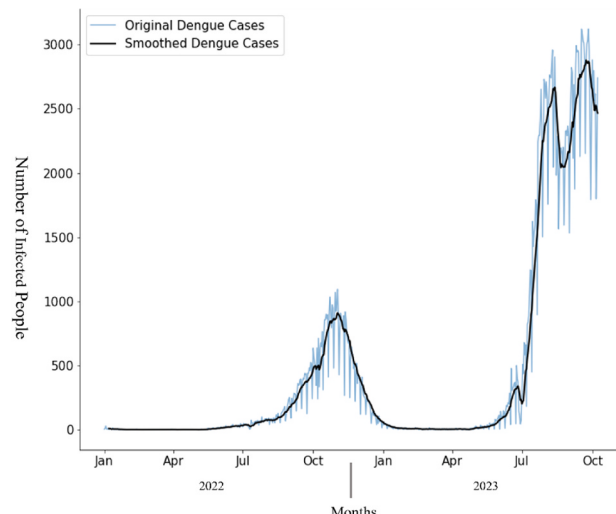


Fig. 10. Visualization depicting the temporal distribution of dengue cases from January 2022 to October 2023. The x-axis denotes the months spanning from January 2022 to October 2023, while the y-axis quantifies the total number of reported dengue cases in Bangladesh.

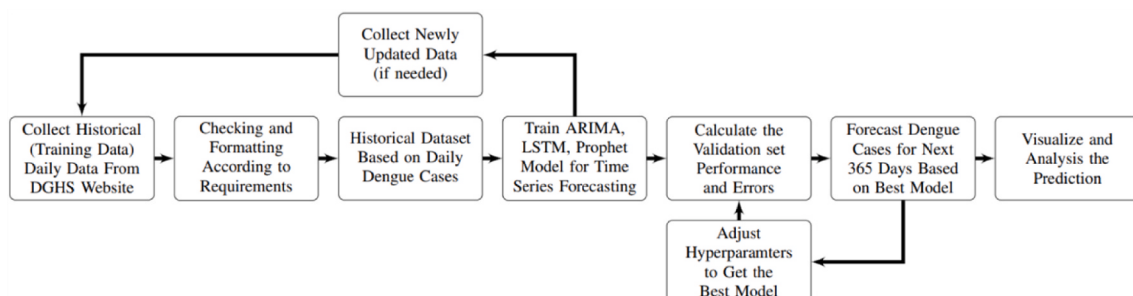


Fig. 9. Workflow for the machine learning-based dengue epidemic forecasting.

Table 5
Hyperparameters of forecasting models.

Method/Model	Parameter	Values
ARIMA	Order (AR, I, MA)	(7, 2, 2)
LSTM	Neurons	50
	Activation	ReLU
	Epochs	100
	Optimizer	RMSProp
	Loss	MSE
Prophet	Changepoints	4
	Yearly Seasonality	True
	Seasonality	Multiplicative
	Changepoint Prior Scale	0.0001

Table 6
Validation set error metrics for all models.

Method/Model	Error Metric	Value
ARIMA	MAE	736.70
	MSE	716123.34
	RMSE	864.24
LSTM	MAE	752.22
	MSE	1096494.11
	RMSE	1047.14
Prophet	MAE	610.09
	MSE	480422.92
	RMSE	693.13

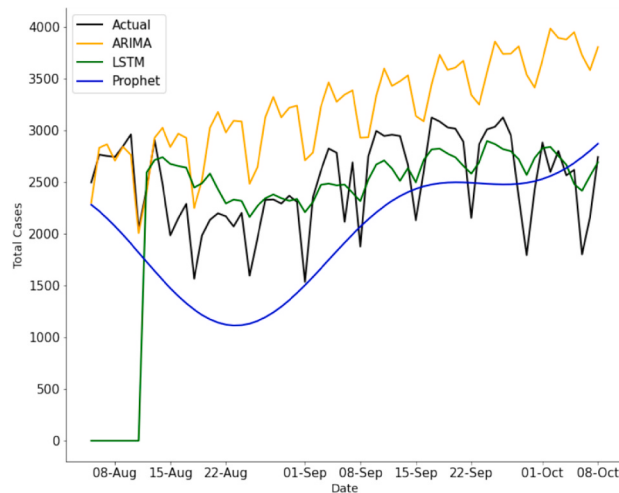


Fig. 11. Comparative Performance of ARIMA, LSTM, and Prophet Models on Validation Set Forecasting from August 5, 2023, to October 8, 2023 (10 % of Training Data), with Mean Absolute Errors (MAE) of 736.70, 752.22, and 610.09, respectively.

yearly seasonality, $h(t)$ encapsulates the effects of holidays accommodating the irregular impact of significant events, and ϵ_t stands as the error term which capturing fluctuations in the data. Notably, we incorporated yearly seasonality with a multiplicative mode and set the number of changepoints to 4. The model was then trained with a changepoint prior scale of 0.0001, providing flexibility in detecting changepoints in the time series.

The details of the hyperparameters used for the three models are in Table 5. Mean absolute error (MAE), mean squared error (MSE), and root mean squared error (RMSE) were computed to evaluate the model's performance, as given in Table 6 [47]. The model performance on the validation set is depicted in Fig. 11, providing a better visual understanding of the model's performance.

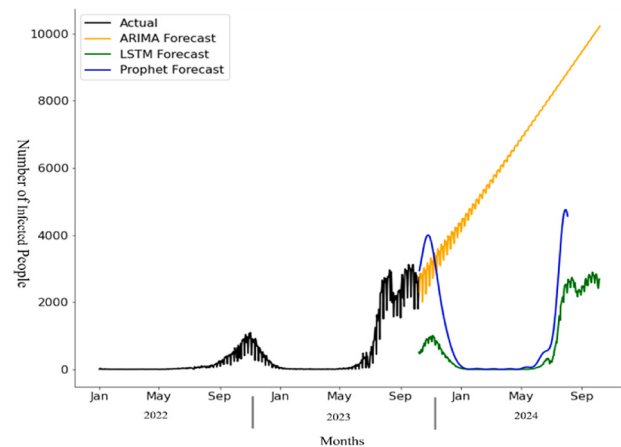


Fig. 12. We have forecasted Dengue cases in Bangladesh from October 2023 to September 2024, utilizing documented data traverse from January 2022 to October 2023. Three distinct forecasting models, ARIMA, LSTM, and Prophet, were employed for comparative analysis, offering insights into their respective predictive performances.

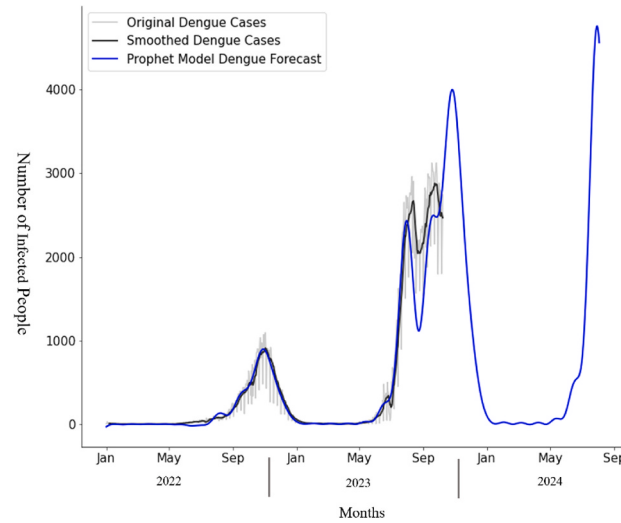


Fig. 13. Results of Forecasted Dengue Cases in Bangladesh using the Prophet model from October 2023 to September 2024, utilizing demonstrated data covering from January 2022 to October 2023.

Our analysis of daily dengue data, depicted in Fig. 10, reveals a significant anomaly post-2021, where unexpected shifts occurred in Bangladesh's dengue trends. Notably, the daily dengue case rate exhibited a multiplicative increase year by year, indicating a pronounced seasonality effect and trend within our dataset. This unforeseen shift often led to periods where the dengue rate remained at zero. Despite ARIMA being one of the most popular statistical time series forecasting models and LSTM's renowned capability to learn intricate patterns, it encountered challenges in adapting to these anomalies, as evidenced by the initial peculiarities observed in the green curve in Fig. 11. However, even though the Prophet curve may not have exhibited exceptional performance, considering the complexity of our data though ARIMA and LSTM may capture some aspects of the data pattern, as shown in Fig. 11, they fail to generalize and accurately represent the trend and seasonality effects observed in our dataset, as evident in Fig. 12., its ability to capture trends is commendable and as mentioned in Table 6 the errors calculated in our work shows the most optimal performance for the Prophet model. So, as seen in Figs. 11 and 12 and the error comparison in Table 6 the limitations of ARIMA and

LSTM in accurately generalizing and capturing the robust trend and seasonality effects present in our dataset is clear in comparison with the Prophet model.

From the accuracy metrics, we find that the Prophet model by Facebook performs the best for our case, with a minimum MAE and RMSE of 610.09 and 693.13, respectively. Furthermore, in our case, the ARIMA statistical model has demonstrated superior performance compared to LSTM, a deep learning model. Although we conducted forecasting for all three models alongside with the forecasting results for the following year as mentioned in Fig. 12. Based on error metrics and feasible scenarios it was evident [48] that the Prophet model captures the seasonality and changepoints in our historical dengue prediction data and closely aligns with feasible values. In addition, it achieved an average accuracy of 85 % on our forecasting task, with a standard deviation of 5 %. These suggest that the model is neither significantly underfitting nor overfitting the data.

Through this fitting, the estimation of the number of individuals likely to be infected in the subsequent day, month, or year can be made [49,50]. The utilization of this information (Fig. 13), can aid in the prevention of the spread of Dengue disease by the Bangladeshi government.

8. Conclusion

In this research, a simplified mathematical model has been developed and can be useful in different regions of the world where seasonal diseases are often experienced. Furthermore, the findings have been examined with the data provided by the IEDCR, a government office that deals with infectious diseases and epidemiology. In our study, a time-dependent transmission rate, denoted as $\beta_H(t)$, was employed due to its significance in understanding Dengue's characteristics over time. The mathematical analysis was focused on in our study, and the existence of positivity and boundedness in our system was proven. Furthermore, based on the equilibria, a basic Reproduction number has been generated, a vital component of the model responsible for different scenario, i.e., endemic or disease-free-equilibria. Several theorems have been proven in our context, utilizing the Ruth-Hurth criteria and ensuring global asymptotic stability.

The development of the Lyapunov function has also been undertaken, demonstrating that our system is globally asymptotically stable. Sensitivity analysis has been employed as well to ascertain the influential parameters that play crucial roles in the spread or diminishment of the disease. Some of the major findings are presented as follows: The infection of mosquito populations is always influenced by β_M , with $\beta_M = 0.5$ being the most-deadliest. For different amplitudes (A) within a sequence of values ($A = 0.1, 0.2, \dots, 0.5$), the highest number of infected mosquitoes occurs in July. However, in the case of the human population, simulations project that when $\beta_M = 0.5$ and $A = 0.1$, the peak of human infections occurs in late September. When A is larger, human infections occur in August or at the beginning of September, with the value $\beta_M = 0.2$. This closely mirrors the actual situation in Bangladesh in the year 2023. It was observed that the solution of the mathematical system is closely tied to the reported infection data by IEDCR, with an estimated correctness of about 85 %. As a result, Fig. 8 depicted an estimation of error.

However, our current model incorporates the impact of seasonal rain on mosquito breeding, focusing on the period between mid-May and late-October when mosquito populations typically rise, leading to a corresponding increase in disease transmission [51]. While this inclusion is a variable step, several other environmental factors can influence mosquito activity and disease spread. Subsequently, controlling Dengue disease is a major concern nowadays; therefore, it could be integrated into the mathematical model for a deeper understanding [52]. Moreover, the vaccination group could be included to study the effect of vaccination on Dengue disease and compare vaccination performance with those who have not received vaccination.

Another issue can be introduced by transition from the current

mathematical model to a more detailed agent-based model [53]. This agent-based model will explicitly represent individual agents, such as humans and mosquitoes, and their interactions within the environment. The agent-based model will incorporate individual characteristics and behaviors of both humans and mosquitoes. We will integrate evolutionary game theory principles into the agent-based framework. This will allow us to model the strategic interactions between humans and mosquitoes as they evolve over time. By exploring these evolutionary dynamics, we aim to identify optimal intervention strategies that can disrupt the transmission cycle and mitigate Dengue outbreaks.

The proposed dynamical model serves as the foundation for capturing the epidemiological dynamics of Dengue disease transmission. The parameters of the model are initially calibrated using historical Dengue incidence data Table 4, allowing us to simulate the spread of the disease over time Fig. 13. The ML component is integrated into our study to enhance the predictive capabilities of the dynamical model and provide more accurate forecasts. Specifically, the outputs of the dynamical model simulations serve as one set of features for training the ML model. Other relevant features include historical Dengue incidence patterns. By leveraging machine learning algorithms, the model can capture nonlinearities and intricate patterns that may not be fully captured by the deterministic model alone. To ensure the coherence and consistency of both models, we rigorously validated and calibrated them using the same historical dataset. These findings can be further developed by the state-of-the-art mechanism namely Transformer based Deep learning could be explored for improved prediction.

We utilize the Prophet model, often employed in seasonal forecasting prediction, to capture complex seasonal patterns. As illustrated in Fig. 10, we observe that the rainy season typically commences in mid-July, reaching its peak from August to October, coinciding with a significant increase in Dengue cases. Subsequently, as rainfall gradually diminishes, the incidence of Dengue cases declines, eventually tapering off to near-zero levels for the remainder of the year. The transmission of infection from one person to another plays a pivotal role in the steady rise of cases over time, culminating in a peak from August to October. Notably, Dengue tends to abate naturally within 8–15 days [54], reflecting the consistently observed patterns. We may predict the number of individuals affected in the upcoming days, weeks, or even months.

CRediT authorship contribution statement

Md Shahidul Islam: Writing – review & editing, Writing – original draft, Visualization, Validation, Supervision, Software, Methodology, Investigation, Formal analysis, Data curation, Conceptualization. **Pabel Shahrear:** Writing – review & editing, Writing – original draft, Validation, Supervision, Resources, Methodology, Investigation, Conceptualization. **Goutam Saha:** Writing – review & editing, Writing – original draft, Visualization, Validation, Software, Formal analysis, Data curation. **Md Ataullha:** Writing – review & editing, Writing – original draft, Visualization, Validation, Software, Methodology. **M. Shahidur Rahman:** Writing – review & editing, Supervision, Software, Conceptualization.

Declaration of competing interest

The authors declare that they have no known competing financial interests or personal relationships that could have appeared to influence the work reported in this paper.

References

- [1] A. Hoffmann, Incompatible mosquitoes, *Nature* 436 (2005) 189, <https://doi.org/10.1038/436189a>.
- [2] S. Sangkaew, D. Ming, A. Boonyasiri, K. Honeyford, S. Kalayanarooj, S. Yacoub, et al., Risk predictors of progression to severe disease during the febrile phase of

- dengue: a systematic review and meta-analysis, *Lancet Infect. Dis.* 21 (7) (2021) 1014–1026, [https://doi.org/10.1016/S1473-3099\(20\)30601-0](https://doi.org/10.1016/S1473-3099(20)30601-0).
- [3] K. Hsan, M.M. Hossain, M.S. Sarwar, A. Wilder-Smith, D. Gozal, Unprecedented rise in Dengue outbreaks in Bangladesh, *Lancet Infect. Dis.* 19 (12) (2019) 1287, [https://doi.org/10.1016/S1473-3099\(19\)30616-4](https://doi.org/10.1016/S1473-3099(19)30616-4).
- [4] A. Wilder-Smith, D.J. Gubler, S.C. Weaver, T.P. Monath, D.L. Heymann, T.W. Scott, Epidemic arboviral diseases: priorities for research and public health, *Lancet Infect. Dis.* 17 (3) (2017) e101–e106, [https://doi.org/10.1016/S1473-3099\(16\)30518-7](https://doi.org/10.1016/S1473-3099(16)30518-7).
- [5] A. Wilder-Smith, E.E. Ooi, O. Horstick, B. Wills, Dengue, *Lancet* 393 (10169) (2019) 350–363, [https://doi.org/10.1016/S0140-6736\(18\)32560-1](https://doi.org/10.1016/S0140-6736(18)32560-1).
- [6] A. Wilder-Smith, J. Hombach, N. Ferguson, M. Selgelid, K. O'Brien, K. Vannice, et al., Deliberations of the strategic advisory group of experts on immunization on the use of CYD-TDV dengue vaccine, *Lancet Infect. Dis.* 19 (1) (2019) e31–e38, [https://doi.org/10.1016/S1473-3099\(18\)30494-8](https://doi.org/10.1016/S1473-3099(18)30494-8).
- [7] S. Banu, W. Hu, Y. Guo, C. Hurst, S. Tong, Projecting the impact of climate change on dengue transmission in Dhaka, Bangladesh, *Environ. Int.* 63 (2014) 137–142, <https://doi.org/10.1016/j.envint.2013.11.002>.
- [8] S. Sharmin, K. Glass, E. Viennet, D. Harley, Interaction of mean temperature and daily fluctuation influences dengue incidence in Dhaka, Bangladesh, *PLoS Neglected Trop. Dis.* 9 (7) (2015) e0003901, <https://doi.org/10.1371/journal.pntd.0003901>.
- [9] O.T. Muurlink, P. Stephenson, M. Islam, A. Taylor-Robinson, Long-term predictors of Dengue outbreaks in Bangladesh: a data mining approach, *Infect. Disease Model.* 3 (2018) 322–330, <https://doi.org/10.1016/j.idm.2018.11.004>.
- [10] O. Dyer, Dengue: Philippines declares national epidemic as cases surge across South East Asia, *BMJ* (Online) 366 (2019) 15098, <https://doi.org/10.1136/bmj.15098>.
- [11] L. Kong, C. Xu, P. Mu, J. Li, S. Qiu, H. Wu, Risk factors spatial-temporal detection for dengue fever in Guangzhou, *Epidemiol. Infect.* 147 (2019) 1, <https://doi.org/10.1017/S0950268818002820>.
- [12] M.S. Hossain, M.H. Siddiquee, U.R. Siddiqi, E. Raheem, R. Akter, W. Hu, Dengue in a crowded megacity: lessons learnt from 2019 outbreak in Dhaka, Bangladesh, *PLoS Neglected Trop. Dis.* 14 (8) (2020) 1–5, <https://doi.org/10.1371/journal.pntd.0008349>.
- [13] S. Islam, C.E. Haque, S. Hossain, J. Hanesiak, Climate variability, Dengue vector abundance and Dengue fever cases in Dhaka, Bangladesh: a time-series study, *Atmosphere* 12 (7) (2021) 905, <https://doi.org/10.3390/atmos12070905>.
- [14] L.L. Xavier, N.A. Honório, J.F.M. Pessanha, P.C. Peiter, Analysis of climate factors and dengue incidence in the metropolitan region of Rio de Janeiro, Brazil, *PLoS One* 16 (5) (2021) e0251403, <https://doi.org/10.1371/journal.pone.0251403>.
- [15] S. Manna, P. Satapathy, I. Bora, B.K. Padhi, Dengue outbreaks in South Asia amid Covid-19: epidemiology, transmission, and mitigation strategies, *Front. Public Health* 10 (2022) 1060043, <https://doi.org/10.3389/fpubh.2022.1060043>.
- [16] S. Naher, F. Rabbi, M.M. Hossain, R. Banik, S. Pervez, A.B. Boitchi, Forecasting the incidence of Dengue in Bangladesh—application of time series model, *Health Sci. Rep.* 5 (4) (2022) 666, <https://doi.org/10.1002/hsr.2066>.
- [17] D. Aldila, M.Z. Ndii, N. Windarto Anggriani, H. Tasman, B.D. Handari, Impact of social awareness, case detection, and hospital capacity on dengue eradication in Jakarta: a mathematical model approach, *Alex. Eng. J.* 64 (2023) 691–707, <https://doi.org/10.1016/j.aej.2022.11.032>.
- [18] S. Hossain, M.M. Islam, M.A. Hasan, P.B. Chowdhury, I.A. Easty, M.K. Tutar, et al., Association of climate factors with Dengue incidence in Bangladesh, Dhaka City: a count regression approach, *Heliyon* 9 (5) (2023) e16053, <https://doi.org/10.1016/j.heliyon.2023.e16053>.
- [19] M.A. Islam, M.N. Hasan, A. Tiwari, M.A.W. Raju, F. Jannat, S. Sangkham, et al., Correlation of dengue and meteorological factors in Bangladesh: a public health concern, *Int. J. Environ. Res. Publ. Health* 20 (6) (2023) 5152, <https://doi.org/10.3390/ijerph20065152>.
- [20] Jafaruddin, S.W. Indratno, N. Nuraini, A.K. Supriatna, E. Soewono, Estimation of the basic reproductive ratio for dengue fever at the take-off period of dengue infection, *Comput. Math. Methods Med.* (2015), <https://doi.org/10.1155/2015/206131>, 2015.
- [21] F. Brauer, C. Castillo-Chavez, A. Mubayi, S. Towers, Some models for epidemics of vector-transmitted diseases, *Infect. Disease Model.* 1 (1) (2016) 79–87, <https://doi.org/10.1016/j.idm.2016.08.001>.
- [22] E.A. Mordecai, J.M. Caldwell, M.K. Grossman, C.A. Lippi, L.R. Johnson, M. Neira, J.R. Rohr, S.J. Ryan, V. Savage, M.S. Shockett, R. Sippy, A.M. Stewart Ibarra, M. B. Thomas, O. Villena, Thermal biology of mosquito-borne disease, *Ecol. Lett.* 22 (10) (2019) 1690–1708, <https://doi.org/10.1111/ele.13335>.
- [23] P.L. Delamater, E.J. Street, T.F. Leslie, Y.T. Yang, K.H. Jacobsen, Complexity of the basic reproduction number (R_0), *Emerg. Infect. Dis.* 25 (1) (2019) 1–4, <https://doi.org/10.3201/eid2501.171901>.
- [24] K.M. O'Reilly, E. Hendrickx, D.D. Kharisma, N.N. Wilastonegoro, L.B. Carrington, I.R.F. Elyazar, A.J. Kucharski, R. Lowe, S. Flasche, D.M. Pigott, R.C. Reiner, W. J. Edmunds, S.I. Hay, L. Yakob, D.S. Shepard, O.J. Brady, Estimating the burden of dengue and the impact of release of wMel Wolbachia-infected mosquitoes in Indonesia: a modeling study, *BMC Med.* 17 (1) (2019) 1–14, <https://doi.org/10.1186/s12916-019-1396-4>.
- [25] Y. Liu, K. Lillepold, J.C. Semenza, Y. Tozan, M.B.M. Quam, J. Rocklöv, Reviewing estimates of the basic reproduction number for dengue, Zika and chikungunya across global climate zones, *Environ. Res.* 182 (January) (2020) 109114, <https://doi.org/10.1016/j.envres.2020.109114>.
- [26] F.M.M. Pereira, P.H.T. Schimit, Spatial dynamics of dengue fever spreading for the coexistence of two serotypes with an application to the city of São Paulo, Brazil, *Comput. Methods Progr. Biomed.* 219 (2022), <https://doi.org/10.1016/j.cmpb.2022.106758>.
- [27] W. Sun, L. Xue, X. Yan, Stability of a dengue epidemic model with independent stochastic perturbations, *J. Math. Anal. Appl.* 468 (2) (2018) 998–1017, <https://doi.org/10.1016/j.jmaa.2018.08.033>.
- [28] N. Izzati Hamdan, A. Kilicman, The development of a deterministic dengue epidemic model with the influence of temperature: a case study in Malaysia, *Appl. Math. Model.* 90 (2021) 547–567, <https://doi.org/10.1016/j.apm.2020.08.069>.
- [29] P. Saha, G.C. Sikdar, U. Ghosh, Transmission dynamics and control strategy of single-strain dengue disease, *Int. J. Dynamic. Control* 11 (3) (2023) 1396–1414, <https://doi.org/10.1007/s40435-022-01027-y>.
- [30] P. Van den Driessche, J. Watmough, Reproduction numbers and sub-threshold endemic equilibria for compartmental models of disease transmission, *Math. Biosci.* 180 (1–2) (2002) 29–48, [https://doi.org/10.1016/S0025-5564\(02\)00108-6](https://doi.org/10.1016/S0025-5564(02)00108-6).
- [31] P. Shahrear, S.M.S. Rahman, Md M.H. Nahid, Prediction and mathematical analysis of the outbreak of coronavirus (COVID-19) in Bangladesh, *Result. Appl. Math.* 10 (2021) 100145, <https://doi.org/10.1016/j.rinam.2021.100145>.
- [32] K. Das, M.N. Srinivas, P. Shahrear, P.S.M. Rahman, Md M.H. Nahid, B.S.N. Murthy, et al., Transmission dynamics and control of COVID-19: a mathematical modelling study, *J. Appl. Nonlinear Dynamic.* 12 (2) (2023) 405–425, <https://doi.org/10.5890/JAND.2023.06.015>.
- [33] M. Bodson, Explaining the Routh-Hurwitz Criterion. A tutorial presentation, *IEEE Control Syst. Mag.* 45 (2020), <https://doi.org/10.1109/MCS.2019.2949974>.
- [34] N. Sharma, R. Singh, J. Singh, O. Castillo, Modeling assumptions, optimal control strategies and mitigation through vaccination to Zika virus, *Chaos, Solit. Fractals* 150 (2021) 111137, <https://doi.org/10.1016/j.chaos.2021.111137>.
- [35] S. Syafuddin, M.S.M. Noorani, Lyapunov function of SIR and SEIR model for transmission of dengue fever disease, *Int. J. Simulat. Proc. Model.* 8 (2–3) (2013) 177–184.
- [36] DGHS, Daily dengue status report, <https://old.dghs.gov.bd/index/php/bd/home/81-english-root/S2020-daily-dengue-status-report>.
- [37] World Health Organization, Dengue Outbreak in Bangladesh, 2023. <https://www.who.int/emergencies/disease-outbreak-news/item/2022-DON424/>. (Accessed 7 October 2023).
- [38] World Health Organization, Disease Outbreak News; Dengue in Bangladesh, 2023. Available at: <https://www.who.int/emergencies/disease-outbreak-news/item/-DON481>.
- [39] D. Zhao, R. Zhang, H. Zhang, et al., Prediction of global omicron pandemic using ARIMA, MLR, and Prophet models, *Sci. Rep.* 12 (2022) 18138, <https://doi.org/10.1038/s41598-022-23154-4>.
- [40] Tzu-Hsin Karen Chen, Vivian Yi-Ju Chen, Tzai-Hung Wen, Revisiting the role of rainfall variability and its interactive effects with the built environment in urban dengue outbreaks, *Appl. Geogr.* 101 (2018) 14–22, <https://doi.org/10.1016/j.apgeog.2018.10.005>. ISSN 0143-6228.
- [41] M.S. Hossain, A.A. Noman, S.A.A. Mamun, et al., Twenty-two years of dengue outbreaks in Bangladesh: epidemiology, clinical spectrum, serotypes, and future disease risks, *Trop. Med. Health* 51 (2023) 37, <https://doi.org/10.1186/s41182-023-00528-6>.
- [42] S. Islam, C.E. Haque, S. Hossain, J. Hanesiak, Climate variability, dengue vector abundance and dengue fever cases in Dhaka, Bangladesh: a time-series study, *Atmosphere* 12 (7) (2021) 905, <https://doi.org/10.3390/atmos12070905>.
- [43] Benjamin Lindemann, Timo Muller, Hanne Vietz, Nasser Jazdi, Michael Weyrich, A survey on long short- term memory networks for time series prediction, in: 2021. 14th CIRP Conference on Intelligent Computation in Manufacturing Engineering, vol. 99, *Procedia CIRP*, 2020, pp. 650–655, <https://doi.org/10.1016/j.procir.2021.03.088>, 15–17, July.
- [44] S.J. Taylor, B. Letham, Forecasting at scale, *Am. Statistician* 72 (1) (2018) 37–45, <https://doi.org/10.1080/00031305.2017.1380080>.
- [45] George EP. Box, Gwilym M. Jenkins, Gregory C. Reinsel, Greta M. Ljung, *Time Series Analysis: Forecasting and Control*, John Wiley & Sons, 2015, <https://doi.org/10.1111/jtsa.12194>.
- [46] A.C. Harvey, S. Peters, Estimation procedures for structural time series models, *J. Forecast.* 9 (1990) 89–108, <https://doi.org/10.1002/for.3980090203>.
- [47] C.A. Faiyaz, P. Shahrear, R.A. Shamim, T. Strauss, T. Khan, Comparison of different radial basis function networks for the electrical impedance tomography (EIT) inverse problem, *Algorithms* 16 (10) (2023) 461.
- [48] Shobhit Chaturvedi, Elangoon Rajasekar, Sukumar Natarajan, Nick McCullen, A comparative assessment of sarima, lstm rnn and fb prophet models to forecast total and peak monthly energy demand for India, *Energy Pol.* 168 (2022) 113097, <https://doi.org/10.1016/j.enpol.2022.113097>.
- [49] P. Shahrear, L. Glass, N. DelBuono, *Analysis of Piecewise Linear Equations with Bizarre Dynamics (Doctoral Dissertation, Ph. D. Thesis, Universita Degli Studio di Bari ALDO MORO, Italy)*, 2015.
- [50] M. Othman, R. Indawati, A.A. Suleiman, M.B. Qomaruddin, R. Sokkalingam, Model forecasting development for dengue fever incidence in surabaya city using time series analysis, *Processes* 10 (11) (2022) 2454, <https://doi.org/10.3390/pr1012454>.
- [51] G. Saha, M. Saha, M. Saha, Dengue: the enduring endemic challenge in Bangladesh, *J. Med.* 25 (1) (2024) 78–82, <https://doi.org/10.3329/jom.v25i1.70530>.
- [52] K.M. Ariful Kabir, M.D. Shahidul Islam, Mohammad Sharif Ullah, Understanding the impact of vaccination and Self-Defense measures on epidemic dynamics using

- an embedded optimization and evolutionary game theory methodology, *Vaccines* 11 (9) (2023) 1421, <https://doi.org/10.3390/vaccines11091421>.
- [53] K.M. Ariful Kabir, M.D. Shahidul Islam, Sabawatara Nijhum, Exploring the performance of volatile mutations on evolutionary game dynamics in complex networks, *Heliyon* 9 (2023) e16790, <https://doi.org/10.1016/j.heliyon.2023e16790>.
- [54] M. Chan, M.A. Johansson, The incubation periods of Dengue viruses, *PLoS One* 7 (11) (2012) e50972, <https://doi.org/10.1371/journal.pone.0050972>.